A SMALL MOLECULE MODULATOR OF HSP90 IMPROVES EXPERIMENTAL DIABETIC NEUROPATHY

BY

Michael J. Urban

B.S. Biology, Benedictine College, 2003
B.A. Chemistry, Benedictine College, 2003

Submitted to the graduate degree program in Medicinal Chemistry and the Graduate Faculty of The University of Kansas in partial fulfillment of the requirements for the degree of Master's of Science.

Thesis Committee:

_____
Brian S.J. Blagg, Ph.D., Chairperson

_____
Thomas E. Prisinzano, Ph.D.

_____
Rick T. Dobrowsky, Ph.D.

Date defended: _____

The Thesis Committee for Michael J. Urban certifies that this is the approved version of the following thesis:

A SMALL MOLECULE MODULATOR OF HSP90 IMPROVES EXPERIMENTAL DIABETIC NEUROPATHY

Thesis Committee:

Brian S.J. Blagg, Ph.D., Chairperson

Thomas E. Prisinzano, Ph.D.

Rick T. Dobrowsky, Ph.D.

Date defended: _____

ABSTRACT

BACKGROUND: Current Hsp90 inhibitors are therapeutically problematic. Although they induce a pro-survival heat shock response that promotes the refolding of damaged proteins, a confounding issue is that at these concentrations the inhibitors are cytotoxic, due to their ability to decrease the maturation of newly synthesized client proteins. KU-32 contains a novobiocin-based scaffold that binds to the C-terminal of Hsp90 and induces a pro-survival heat shock response at a concentration ~10,000 fold lower than that needed to induce neurotoxicity. This creates an optimal therapeutic window in which to operate, providing promise towards the development of novel neuroprotective agents.

OBJECTIVE: To evaluate whether the induction of the heat shock response through Hsp90 modulation could decrease or reverse the pathophysiological progression of diabetic peripheral neuropathy in Type-1 diabetic mice.

HYPOTHESIS: A small molecule modulator of Hsp90 will improve experimental diabetic neuropathy.

METHODS: After 8-12 weeks of diabetes induced by streptozotocin, the effects of weekly doses of KU-32 on several standard indices of diabetic neuropathy were measured.

RESULTS: Initial toxicity studies employing the weekly intraperitoneal administration of 2 or 20 mg/kg KU-32 to non-diabetic mice over 6 week duration did not alter motor or sensory nerve conduction velocity (MNCV/SNCV), mechanical or thermal sensitivity, or intra-epidermal nerve fiber density. Thus, the drug alone had no effect on altering common measures of neuropathy. In a 12-week intervention study, wild-type C57 Bl/6 animals receiving a weekly treatment regimen of 20 mg/kg KU-32 for 6 weeks exhibited a steady recovery to control levels in thermal and mechanical sensitivity, MNCV, and SNCV. KU-32 did not alter metabolic control. As Hsp70 is hypothesized to be a major target for KU-32, its necessity in neuroprotection was examined using Hsp70 double knockout mice (Hsp70.1/Hsp70.3). In a 12-week intervention study, Hsp70 knockout mice receiving a weekly treatment regimen of 20 mg/kg for 6 weeks displayed no improvements in thermal and mechanical sensitivity, MNCV, and SNCV. In 8-week intervention studies, animals demonstrated recoveries in sensory hypoalgesia and nerve conduction velocity deficits in a dose-dependent manner. KU-32 did not alter sensory nerve fiber innervation.

CONCLUSIONS: These data suggest that hyperglycemia may adversely impact the ability of neurons to promote refolding or decrease unfolding of mildly damaged proteins. C-terminal Hsp90 modulators can improve several standard clinical indices of negative symptoms associated with small and large fiber dysfunction in the absence of improving overall metabolic control. The affects of KU-32 appear to be dose-dependent and require the presence of inducible Hsp70 for efficacy. Inducible Hsp70 is not required for the pathophysiological progression of diabetic neuropathy.

ACKNOWLEDGEMENTS

Most importantly, I must thank God for protecting and watching over me during my deployment to Operation Iraqi Freedom and enabling my safe return. Without which, I wouldn't be here today. To the love of my life, Katie Urban, and our two boys, Joseph and Erik, thank you for all your patience, faith, and unwavering love and support throughout my journeys. I wouldn't be where I am today or be able to do what I do without your love and support.

I'd like to thank my advisor Dr. Brian Blagg for your mentorship, faith in my abilities, and willingness to take me under your wing as a biochemist graduate student working in a predominately organic synthesis lab. Thank you for entrusting me with such a demanding and rewarding project while allowing the freedom to explore and excel. Thank you to my collaborator, Dr. Rick Dobrowsky, whose invaluable guidance, technical expertise, and mentorship have molded and established my current knowledgebase and inspired me to pursue a career in developing therapeutics to treat neurological disorders.

To my parents, Joseph and Carol Urban, I am so grateful for all the faith, love, and encouragement you have provided throughout my life and my career. Thanks to my siblings Jeremy, Joshua, and Audra for your friendship, love, support, and development of my competitive streak. I have learned so much about myself through you.

I must thank all my friends, mentors, and leadership within the U.S. Army and the Kansas Army National Guard for their continued flexibility, understanding, and

willingness to let me pursue my civilian career and better serve my country through scientific achievement.

I would like to thank all of the Blagg and Dobrowsky lab members for all the many roles they have played in my scientific development. I would like to specifically thank Dr. James McGuire, Dr. Cuijuan (Melanie) Yu, and Liang Zhang for their contributions to my work and education.

Finally, I'd like to thank Dr. Thomas E. Prisinzano and Dr. Rick T. Dobrowsky for their time in serving on my thesis committee.

This work was made possible by the funding from the National Institutes of Health and the Juvenile Diabetes Research Foundation.

TABLE OF CONTENTS

LIST OF FIGURES

LIST OF TABLES

LIST OF ABBREVIATIONS

ABC	avidin-biotin complex
ACE	angiotensin-converting enzyme
ADA	American Diabetes Association
ADP	adenosine diphosphate
AGEs	advanced glycation endproducts
AIDS	acquired immunodeficiency syndrome
ANOVA	analysis of variance
AR	aldose reductase
ATP	adenosine triphosphate
BAG-1	Bcl-2-associated athanogene
Bax	Bcl-2–associated X
BBB	blood-brain barrier
Ca^{2+}-CaM	calcium-calmodulin
CDC	Center for Disease Control and Prevention
CHIP	carboxyl-terminus of Hsc70/Hsp70-interacting protein
c-Met	cellular MNNG (N-Methyl-N'-nitro-N-nitroso-guanidine) HOS Tranforming gene
CSII	continuous subcutaneous insulin infusion
CSPα	cysteine string protein-α
DAG	1,2-Diacylglycerol
DCCT	Diabetes Control and Complications Trial
DNA	deoxyribonucleic acid
DPN	diabetic polyneuropathy/peripheral neuropathy
DPN	diabetic peripheral neuropathy
DPP	Diabetes Prevention Program
DRG	dorsal root ganglia
DRPLA	dentatorupallidolysian atrophy
EDTA	ethylenediaminetetraacetic acid

ELISA	enzyme-linked immunosorbent assay
eNOS	endothelial nitric oxide synthase
ER	endoplasmic reticulum
FAD	flavin adenine dinucleotide (oxidized)
$FADH_2$	flavin adenine dinucleotide (reduced)
FAK	focal adhesion kinase
FBG	fasting blood glucose
GAK	cyclin G-associated kinase
GD	gestational diabetes
GEF	guanonucleotide exchange factor
GLUT	glucose transporter
GPCRs	G-protein coupled receptors
Grp94	glucose-regulated protein-94
GSH	glutathione (reduced)
GSSG	glutathione (oxidized)
$G_{\alpha s}$	G-stimulative α subunit
HbA_{1C}	glycated hemoglobin
HIV	human immunodeficiency virus
HRP	horseradish peroxidase
Hsc70	heat shock cognate-70
HSEs	heat shock elements
HSF-1	heat shock factor-1
Hsp	heat shock protein
HSP70 KO	Hsp70.1/Hsp70.3 double knockout
HSR	heat shock response
IACUC	Institutional Animal Care and Use Committee
IENFD	intraepidermal nerve fiber density
IL-1β	interleukin-1β
iNOS	inducible nitric oxide synthase

IP	intraperitoneal
K_M	Michaelis constant
LC-MS/MS	liquid chromatography-mass spectrometry/mass spectrometry
LDL	low-density lipoprotein
MNCV	motor nerve conduction velocity
mRIPA	modified radioimmunoprecipitation assay
mtHsp70	mitochondrial Hsp70
mtt	mutant huntingtin
NAD+	nicotinamide adenine dinucleotide (oxidized)
NADH	nicotinamide adenine dinucleotide (reduced)
NADP+	nicotinamide adenine dinucleotide phosphate (oxidized)
NADPH	nicotinamide adenine dinucleotide phosphate (reduced)
NCV	nerve conduction velocity
NF-κB	nuclear factor kappa-light-chain-enhancer of activated B cells
NIH	National Institutes of Health
nNOS	neuronal nitric oxide synthase
NOHLA	N^{ω}-hydroxyl-L-arginine
NOS	nitric oxide synthase
NRG-1	neuregulin-1 type II
NSAIDs	non-steroidal anti-inflammatory drugs
***O*-GlcNAc**	*N*-acetyl-D-glucosamine
OGT	*O*-GlcNAc transferase
PAI-1	plasminogen activator inhibitor-1
PARP	poly(ADP-ribose) polymerase
PBS	phosphate buffered saline
PBS-T	PBS-tween
PKC	protein kinase-C
PKC-β	protein kinase-C-β
PKG	protein kinase-G

PrP^{C}/PrP^{Sc}	cellular prion protein/scrapie prion protein
PTM	post-translational modification
RAGE	receptor for AGE
Rme-8	receptor-mediated endocytosis-8
RNS	reactive nitrogen species
ROS	reactive oxygen species
RVLM	rostral ventrolateral medulla
S	serine
SAR	structure-activity relationship
SAXS	small-angle X-ray scattering
SC	Schwann cell
SCA	spinocerebellar ataxias
SC-DRG	Schwann cell-dorsal root ganglia
SDH	sorbitol dehydrogenase
SDS-PAGE	sodium dodecyl sulfate-polyacrylamide gel electrophoresis
SEM	mean standard error
SMBA	spinal and bulbar musclular atrophy
SNARE	Soluble *N*-ethylmaleimide-sensitive factor Attachment protein Receptors
SNCV	sensory nerve conduction velocity
SOD	superoxide dismutase
SSNRIs	serotonin–norepinephrine reuptake inhibitors
SSRIs	selective serotonin reuptake inhibitors
STZ	streptozotocin
T	threonine
T1DM	type 1 diabetes mellitus
T2MD	type 2 diabetes mellitus
TCA	tricarboxylic acid
TCAs	tricyclic antidepressants
TF	transcription factor

TGF-β	transforming growth factor-β
TMZ	3,3',5,5'-tetramethylbenzidine
TNF-α	tumor necrosis factor-α
TOM70	translocase of the outer membrane-70
TRAP-1	tumor necrosis factor receptor associated protein-1
UDP-*O*-GlcNAc	uridine diphosphate-*N*-acetyl-D-glucosamine
UV-Vis	ultraviolet-visable
VEGF	vascular endothelial growth factor
VEGFR	VEGF receptor
veh	vehicle
WT	wild-type
Y	tyrosine

CHAPTER 1: INTRODUCTION

I. DIABETES MELLITUS

The severe complications associated with diabetes mellitus will lead to nearly four million deaths worldwide in 2010.[1] Diabetes has become an epidemic, demanding the attention and recognition of the United Nations as the first non-infectious disease to pose a serious international health threat, comparable to infectious diseases (*e.g.* HIV/AIDS, tuberculosis, and malaria).[1-2] The prevalence of diabetes within the global population is projected to increase from 7.9% to 8.4% by 2030, affecting 439 million people.[1]

In 2007, the United States spent $174 billion towards the medical treatment of 17.9 million diabetic patients, while an additional 6.6 million remained undiagnosed or untreated.[1, 3-6] In fact, since 2002, the number of diagnosed diabetics in the U.S. has steadily increased at an alarming rate of one million each year. The Center for Disease Control and Prevention's (CDC's) last report was in 2008, bearing 18.8 million diagnoses (6.3% of the U.S. population).[4, 7]

Despite its prominence in today's society, there are very few therapeutic options available to treat diabetes and its associated complications. Although controlled insulin therapy significantly decelerates the rate of diabetes progression, acute and chronic diabetic complications still develop, deteriorating individual health to the point of lethality. Most of the current therapeutics addressing diabetic complications are geared towards symptomatic relief.[8-17] This is especially true in the treatment of the diabetic neuropathies. In order to better understand the current

treatment regimens and the potential for therapeutic advancement against diabetic neuropathy, an examination of the disease's influence on neurodegeneration will be conducted. A novel, multifaceted approach is needed to adequately mitigate and reverse the onset and progression of diabetic peripheral neuropathy.

II. NEUROPATHOPHYSIOLOGY

The Diabetes Control and Complications Trial (DCCT, 1983-1993) marked an important milestone in establishing the etiology of diabetic complications. The study provided the first compelling evidence to support the hypothesis that hyperglycemia directly contributes to the development and progression of diabetes mellitus associated complications (*i.e.* neuropathy, nephropathy, retinopathy).[18] Diabetic peripheral neuropathy is the attrition of nerve fibers within the somatic and autonomic nervous systems through altered glucose metabolism resulting from hyperglycemia. It is estimated that 60-70% of all diabetics will experience some form of neuropathy throughout the course of their disease.[5] The mechanisms by which hyperglycemia induces neurotoxicity will be addressed in the subsequent "Glucose Neurotoxicity" section. However, to better understand how glucose accumulates at toxic levels within the neurons, the primary means of systemic blood glucose absorption must be examined.

Glucose Accumulation in Neurons

Glucose is transported across cellular membranes through glucose transporters (GLUTs). This family of solute carriers contains several isoforms that are distributed throughout the body by tissue type. Neuronal glucose accumulation involves

abnormal changes in the GLUT1, GLUT2, GLUT3, and GLUT4 isoforms as the result of altered endocrine signaling. Under normal physiological conditions, transient increases in blood-glucose levels trigger the release of insulin, a polypeptide hormone secreted by β-cells in the pancreatic islets of Langerhans.[19-20] Insulin binds to insulin receptors in hepatic, muscle (skeletal and cardiac), and adipose cell membranes.[21-23] This binding induces an intracellular signaling cascade that shuttles GLUT-4 glucose transporters (stored in vesicles) to the plasma membrane where they facilitate glucose uptake.[24-25] GLUT-4 transporters serve as the body's primary mechanism to absorb and clear glucose from the blood. If the insulin signal is destroyed, or the signaling cascade is compromised (*e.g.* acquired insulin resistance/tolerance), systemic glucose levels rise and these tissues become malnourished and can no longer sustain normal physiological activity.[25]

In contrast, the nervous system cannot afford sporadic or sustained periods of glucose deprivation and employs insulin-insensitive GLUT-1 and GLUT-3 glucose transporters to transport extracellular glucose.[25-29] GLUT-1 facilitates glucose transport across endothelial cells of the blood-brain barrier (BBB), while GLUT-3 facilitates transport across various tissues in the central and peripheral nervous systems.[25-26, 28] As the source of insulin secretion, the pancreas must employ its own constitutively active GLUT-2 glucose transporters as well.[25, 28, 30] When pancreatic glucose concentrations reach a certain threshold, the β-cells secrete insulin to cue muscle, fat, and liver to help clear excess glucose.[25, 28] However, in type 1 diabetes, sustained hyperglycemia overwhelms the β-cells and causes them to shut down,

reducing insulin secretion and insulin-induced glucose absorption. Without the insulin-activated GLUT-4 to assist in systemic clearance, glucose seeps into the neurons unregulated at an abnormally high rate. To compound this problem, insulin also stimulates glycogen synthesis and storage in the liver via activation of glycogen synthase.[25] In the absence of insulin, glycogen synthesis fails and gluconeogenesis pursues, releasing yet more glucose into the blood and increasing flux into the neurons. This extra release in glucose serves as a compensatory mechanism to mitigate alleged, systemic "starving" conditions detected by hepatocytes.[25] Overall, the deterioration of insulin signaling increases blood glucose levels by decreasing the activation of glucose transporters in adipose/muscle tissue and increasing gluconeogenesis. This increase in blood-glucose concentrations drives more glucose into the nerves, increasing metabolic flux via glucose metabolism, which contributes to neurotoxicity.

The underlying causes behind insulin degeneration and insensitivity differ within all three major forms of diabetes: Type 1, Type 2, and Gestational. Type 1 diabetes mellitus (T1DM), which used to be referred to as "juvenile diabetes," usually develops early in life, comprising 5-10% of all diabetic cases.[4-6, 10, 16, 31] This condition typically arises when the patient's autoimmune system targets and destroys β-cells, eliminating the individual's source of insulin.[4-6, 10, 16, 31-32] Approximately 80% of Type 1 diabetics express islet cell antibodies that selectively target β-cells for immune-mediated elimination.[10] Some patients also produce autoantibodies against insulin and other endocrine tissues such as the adrenal, thyroid, and parathyroid

glands.[10] Although the root cause remains to be determined, a significant environmental influence has become evident through identical twin studies.[32] Twin studies are the classic argument to evaluate exclusive genetic predisposition as both twins share identical genotypes and should ideally express the same phenotypes (*i.e.* diabetes) throughout life. In documented diabetic cases involving identical twins, the likelihood of both twins contracting the disease is about 50%.[33-36] These twin studies refute an exclusive genetic basis for type 1 diabetic disease development. Intriguingly, a small fraction of Type 1 diabetics are void of any autoimmune factors, but yet still display clear signs of hypoinsulinism.[16, 32] The disease etiology behind these idiopathic diabetics remains unknown. Nevertheless, this sect of type 1 diabetics cannot sufficiently produce enough insulin to alleviate neuronal hyperglycemia.[16, 32] In general, type 1 diabetes arises either through β-cell incapacitation/dysfunction (affecting the production and secretion of insulin) or through systemic insulin elimination during circulation.

In contrast to type 1, type 2 diabetes mellitus (T2DM) typically develops towards the later stages of life, accounting for nearly 90% of all diabetic patients.[4-5, 34] In T2DM, the patient either develops deficits in insulin production/secretion or acquires a resistance to negate insulin efficacy (*e.g.* impaired insulin signaling).[4-5, 31-32] T2DM exhibits a relatively higher genetic predisposition in comparison to T1DM, often exhibiting mutations in genes associated with insulin secretion or intracellular signaling, such as glucokinase or Akt-2, respectively.[32, 37] Typically, the consequences of these mutations go unnoticed early in life as the body slowly makes

adjustments to mitigate these shortcomings, such as increasing insulin production or overexpressing other intracellular signaling proteins to increase pathway sensitivity. However, these genetic defects compound over time and under physiological stress. The Diabetes Prevention Program (DPP, 1998-2001) determined that increasing age, obesity, and sedentary lifestyle significantly increase the development of Type 2 diabetes.[38] Controlled exercise and low-fat diets decreased the mean body weight by 5-7% and the onset of Type 2 diabetes by 58%.[38] To summarize, type 2 diabetes manifests itself in the later stages of life, and is associated with an increasingly sedentary lifestyle and obesity. Sedentary lifestyles, obesity, and time exacerbates an already stressed intracellular (*i.e.* β-cell, adipocyte, and muscle cell) metabolic state acquired through genetic predisposition. Collectively, these factors reduce/halt insulin secretion and sensitivity, debilitating GLUT4 glucose transporters and, thus, increasing neuronal metabolic demand.

Gestational Diabetes (GD) occurs when glucose intolerance arises during the third trimester of pregnancy, affecting 4% of U.S. pregnancies annually.[32] GD is triggered by pregnancy-induced metabolic alterations that results from maternal nutritional irregularities (*i.e.* glucose) associated with fetal nourishment.[4-5, 32] The etiology of GD is very similar to type 2 diabetes and the risk of contraction is generally higher in obese women, individuals with a family history of diabetes, and certain ethnic groups. If untreated, the disease can endanger the fetus and the mother.[4-5, 32] Approximately 5-10% of the mothers with GD will become Type 2 diabetic postpartum, while the chances of developing Type 2 within the next ten years (postpartum) is 40-60%.[4-5, 32]

Similar to type 2 diabetes, gestational diabetes occurs during stressful physiological conditions (pregnancy) that increase or cause significant fluctuations in metabolic demand. Consequently, GD amplifies preexisting metabolic abnormalities that diminishes insulin secretion, weakens insulin sensitivity, and increases neuronal burden.

Despite their different etiologies, each type of diabetes generates hyperglycemic conditions that systemically alter the individual's metabolic state, producing severe acute and chronic complications. These complications include peripheral neuropathy, cardiovascular disease, retinopathy, and nephropathy.[18, 25, 28, 38] Although hyperglycemia primarily drives neurodegeneration, several of the other diabetic complications feed neuropathic development, amplifying its progression. These other complications will be discussed briefly in the context of neuropathic development in the proceeding section. Thus far, only the means of neuronal glucose accumulation have been discussed. The specific mechanisms by which glucose induces toxicity will be examined below.

Glucose Neurotoxicity

Hyperglycemia instills its neurotoxic effects primarily through metabolic congestion. As the cell is forced to employ contingency plans to metabolize excess glucose, intracellular coenzyme and antioxidant supplies (*e.g.* NAD^+, NADPH, Glutathione) quickly deplete. As time progresses, the neurons reroute critical coenzyme and antioxidant supplies to support more crucial, life-sustaining functions. Ironically, failure to properly supply any of these metabolic pathways leads to cellular

demise. These chokepoints arise within glycolysis, the tricarboxylic acid (TCA) cycle, polyol (sorbitol) pathway, and hexosamine pathway, inducing oxidative/nitrosative stress, inflammation, and glycemic post-translational modifications that alter protein expression and function. Each of these metabolic pathways and their instilled physiological consequences will be addressed.

Glycolysis and TCA Cycle

The neuronal response to increased glycemic concentrations is to upregulate the main and alternate metabolic pathways. The first line of defense is to increase glucose flux through glycolysis, followed by subsequent entry into the TCA Cycle (Figure 1.1). Several of these metabolic steps employ the oxidizing coenzymes NAD^+ (nicotinamide adenine dinucleotide) and FAD (flavin adenine dinucleotide), which reduce to NADH and $FADH_2$, respectively.[39] Each molecule of glucose typically yields ten molecules of NADH and two $FADH_2$.[39] These reduced coenzymes undergo oxidative phosphorylation in the mitochondria to collectively yield 26-28 molecules of ATP (adenosine triphosphate).[39] However, the problem herein lies with the rapid saturation of hexokinase (glucokinase), which quickly surpasses its capabilities.[17, 25] This is compounded by the fact that hexokinase is often mutated in type 2 diabetics (discussed previously). As the capacities of hexokinase are exceeded, the neuron must implement contingency plans to shunt excess glucose into relatively minor metabolic pathways of glucose metabolism. These metabolic contingency plans normally consist of the polyol and hexosamine pathways.

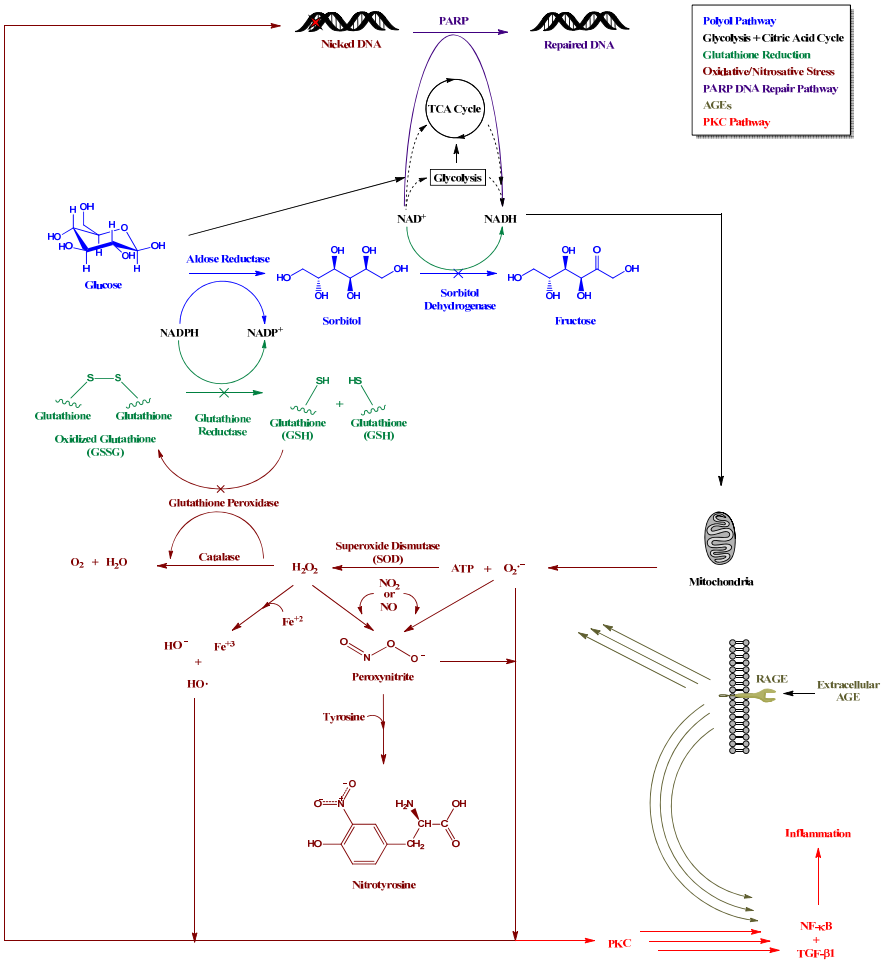

Figure 1.1. Metabolic demands in hyperglycemic neurons.

Polyol (Sorbitol) Pathway

The polyol, or sorbitol pathway, provides the majority of reinforcing support to glycolysis and the TCA cycle (Figure 1.1). With glucose levels typically four times higher in diabetics than normal, hexokinase becomes overwhelmed and glucose concentrations quickly approach the K_M of aldose reductase (AR) (*n.b.* glucose binding affinities: AR << hexokinase).[25] Aldose reductase utilizes the coenzyme NADPH (nicotinamide adenine dinucleotide phosphate) to reduce glucose to sorbitol.[17, 25, 40] Under less stringent conditions, sorbitol oxidizes to fructose via

sorbitol dehydrogenase (SDH) and NAD^+.[40] However, the bulk of NAD^+ stock is depleted during glycolysis and the TCA cycle, resulting in sorbitol accumulation. The formation of sorbitol drains reserve NADPH stockpiles, a coenzyme required for glutathione reductase to convert oxidized glutathione (GSSH) back to glutathione (GSH).[17, 25, 41] Without reduced glutathione, cellular defenses against oxidative/nitrosative stress (discussed below) weaken. The surplus of hydrophilic, impermeable sorbitol arguably alters intracellular osmolarity, inducing swelling.[17, 25, 40-41] To compensate, neurons alter internal osmolyte (*e.g.* myo-inositol) concentrations to reduce osmotic pressure.[17, 25, 41-42] Myo-inositol is an important precursor to an assortment of secondary messengers within various signaling pathways.[42] However, without sound evidence, the generation of osmolar and myo-inositol irregularities in diabetic neuropathy remains debatable. Regardless, aldose reductase provides an alternate means to metabolize excess glucose upon hexokinase saturation. Unfortunately, NADPH employment by AR inhibits the recycling of functional glutathione needed to neutralize the increasing oxidative and nitrosative insults in neurons (discussed below).

Oxidative and Nitrosative Stress

The depletion of functional glutathione and the increase in NADH with glycolysis/TCA cycle has serious repercussions in mitochondrial operations. During oxidative phosphorylation, O_2 is usually reduced to H_2O. However, a small percentage (1-4%) isn't completely reduced and, instead, forms the free radical byproduct superoxide, $O_2^{\cdot -}$ (Figure 1.1).[25, 40-41] The mitochondrial protein SOD

(superoxide dismutase) normally converts this reactive oxygen species (ROS) to H_2O_2, where catalase reduces it to H_2O and O_2.[41] This conversion is normally reinforced by glutathione peroxidase, glutathione *S*-transferase, and thioredoxin. However, all of these proteins require either NADPH or reduced glutathione to reduce H_2O_2.[25, 41] H_2O_2 reacts with iron (II) to generate iron (III), hydroxide, and hydroxyl radicals (Fenton and Haber-Weiss reactions) and with nitrite to form the reactive nitrogen species (RNS) peroxynitrite ($ONOO^-$).[25, 41] Peroxynitrite also forms when nitric oxide, an abundant neurotransmitter produced by nitric oxide synthase, reacts with superoxide. Under hyperglycemic conditions, mitochondria produce relatively large quantities of ROS/RNS.[41] These toxic free radicals escape the mitochondria, drain the cellular antioxidant defense mechanisms, and can modify cellular components (*e.g.* proteins, membranes, DNA).[17, 41] One common indicator of RNS protein modification is the nitrosylation of tyrosine residues upon interaction with peroxynitrite, yielding nitrotyrosine. ROS/RNS-induced genetic modifications become irreparable as many of the cell's DNA repair mechanisms such as PARP (poly(ADP-ribose) polymerase) must compete for exhausted NAD^+.[40] Redirecting NAD^+ to assist in genetic repairs deters glycemic clearance, leading to further glucose accumulation. The battle for coenzymes to maintain homeostatic conditions is a lose-lose situation.

Hexosamine Pathway and Advanced Glycation Endproducts (AGEs)

Another contingent mechanism to deal with profuse amounts of glucose is the hexosamine pathway, which diverges from glycolysis after the conversion of glucose

6-phosphate to fructose 6-phosphate (Figure 1.2). The hexosamine pathway generates an abundance of uridine diphosphate-*N*-acetyl-D-glucosamine (UDP-*O*-GlcNAc). *O*-GlcNAc transferase (OGT) utilizes this metabolite to post-translationally modify (*O*-GlcNAcylate) several key signaling proteins and transcription factors.[25, 43-44]

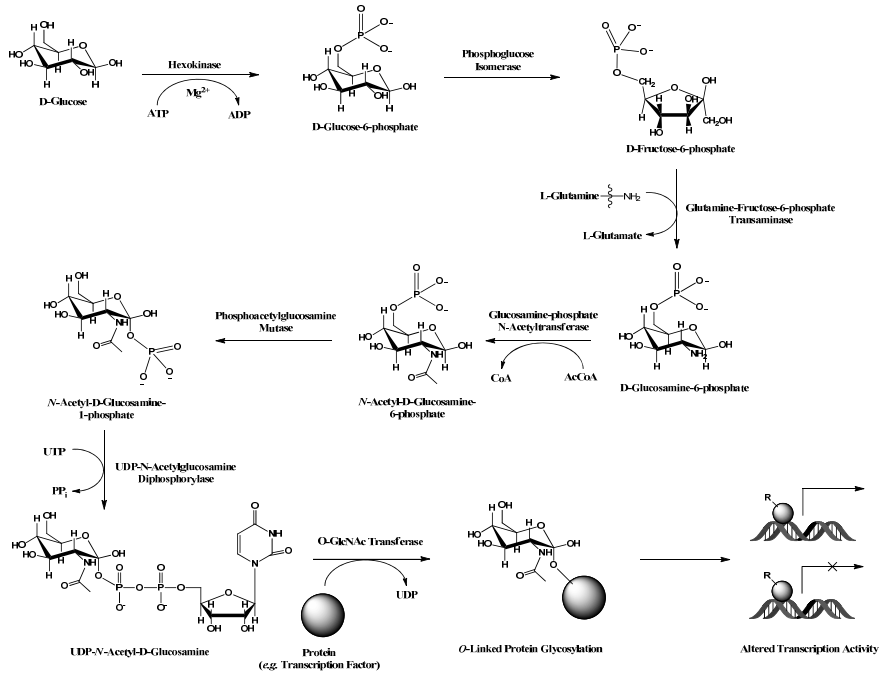

Figure 1.2. *O*-GlcNAcylation of proteins through the hexosamine pathway.

Intriguingly, all known proteins that undergo *O*-GlcNAcylation can also be phosphorylated (*e.g.* p53, c-*myc*, estrogen receptor, and YY1).[45-49] Mounting evidence supports extensive cross-talk between *O*-GlcNAcylation and phosphorylation, revealing both negative and positive modulation of phosphorylation regulatory effects.[44-45, 50] Phosphorylation regulates several cellular processes, including intracellular signaling cascades, transcription factors, and cellular trafficking essential to cell growth and survival. Abnormalities in phosphorylation and *O*-GlcNAcylation states have been implicated in diabetes and cancer; this typically arises due to changes

in flux through the hexosamine pathway, unmanaged kinase activity, or mutations in protein regulatory sites. For example, *O*-GlcNAcylation of the tumor suppressor p53 induces the expression and phosphorylation of p53, preventing proteolytic degradation (of p53) and inducing pro-apoptotic gene transcription.[49, 51] Transcription factors (TFs), such as c-*myc*, are often upregulated and phosphorylated during cancerous activity, enabling the transcription of pro-survival oncogenic proteins.[47, 49, 51] *O*-GlcNAcylation of the c-*myc*'s phosphorylation site inhibits phosphorylation and negates TF activation, indicating a "Yin-Yang" regulatory model.[47] *O*-GlcNAcylation also increases the turnover/degradation of the estrogen receptor (normally upregulated/hyperactive in several breast cancers), indicating a significant effect upon signal transduction as well.[46] *O*-GlcNAcylation also impacts client protein recognition and function of several molecular chaperones/co-chaperones within the heat shock family (addressed in subsequent Hsp70 and Hsp40 section). Hence, excessive *O*-GlcNAcylation under hyperglycemic stress can severely disrupt the neuron's homeostatic state (transcription, signal transduction, and trafficking activity), generating adverse survival conditions.

In addition to *O*-GlcNAcylation, non-enzymatic protein glycosylation is common under hyperglycemic conditions, yielding stable AGEs (advanced glycation endproducts) by the Amadori Rearrangement.[17, 25, 40-41, 52-54] In AGE formation (Figure 1.3), the primary amine of arginine's δ-guanidino group (or lysine's ε-amino group) attacks the anomeric carbon of glucose.[52-53] The anomeric oxygen then becomes protonated and the free electron pair of the secondary amine attacks the

adjacent carbon, forming a Schiff base and releasing H_2O. Upon deprotonation of the charged nitrogen, subsequent deprotonation at the C-2 position affords the enolate, regenerating the secondary amine .[52-53] Tautomerization gives the ketone product which can undergo cyclization to yield the Amadori complex, or AGE.[52-53]

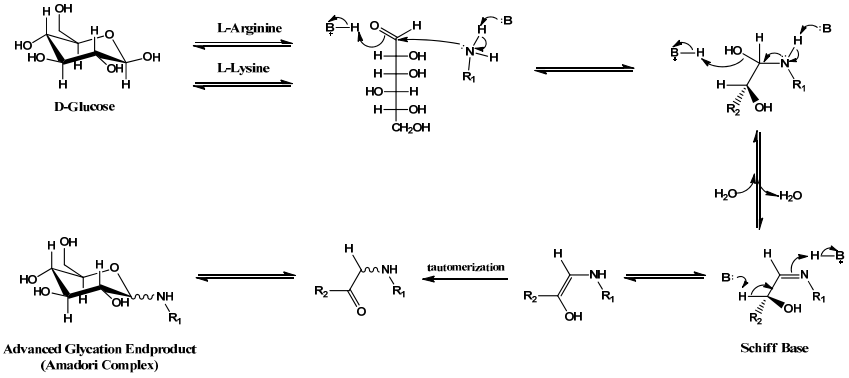

Figure 1.3. Formation of AGEs through the Amadori Rearrangement.

This glycoxidation permanently alters all encountered protein components within or supplying the peripheral nervous system (*e.g.* myelin proteins, neuronal cytoskeletal proteins, extracellular matrix proteins, and supporting microvasculature).[17, 55-56] Extracellular AGE can bind to RAGE (receptor for AGE), inducing the activation of nuclear transcription factor NF-κB (Figure 1.1) in dorsal root ganglia (DRGs) neurons. Activation of the AGE-RAGE-NF-κB pathway further induces ROS formation, nuclear DNA degradation, and caspase-3-mediated apoptosis .[55-56] NF-κB also induces the release of the proinflammatory cytokines TNF-α (tumor necrosis factor-α) and IL-1β (interleukin-1β), inducing neuronal apoptosis (and decreasing sensation) or increasing pain, respectively.[55, 57]

The most common AGE readily measured in diabetics is glycated hemoglobin (HbA_{1C}).[54] Specialized HbA_{1C} indicators, similar to blood-glucose meters, can easily

detect percent HbA_{1C} levels from a small blood sample. In 2010, the ADA published diagnosis guidelines establishing diabetic HbA_{1C} levels at ≥ 6.5% (48 mM) versus normal levels at 5-6% (31 mM) in humans; these levels match the percentages observed in experimental murine models.[58]

Protein Kinase-C (PKC) Pathway

Under hyperglycemic conditions, glyceraldehyde-3-phosphate (glycolysis) can be diverted to form 1,2-Diacylglycerol (DAG). DAG activates several PKC isoforms (*n.b.* PKC-β), altering the expression of various angiogenic proteins (VEGF (vascular endothelial growth factor) and PAI-1 (plasminogen activator inhibitor-1)) and proinflammatory/proapoptotic proteins (NF-κB and TGF-β (transforming growth factor-β)).[41, 59] PKC-β inhibitors (*i.e.* LY333531) show substantial improvements in motor nerve conduction velocity.[59-60] However, this recovery is most likely due to improvements in vascular support, providing a temporary patch towards an increasingly complex problem.

Hyperlipidemia and Neurodegeneration

Additional microvascular dysfunction to the *vasa nervorum* (blood vessels supplying the nerves) stems from adipose starvation. Adipose starvation triggers lipolysis, allowing free fatty acids to filter into the blood, enter the liver, and undergo β-oxidation.[61-63] Up to 97% of all diabetics display at least one abnormal fatty acid level in the blood.[64-65] Hyperlipidemia generates small lipoprotein molecules, predominately LDL-cholesterol, that bind to arterial walls, decreasing plasticity.[65] This primes the arteries to develop hardening plaques, leading to atherosclerosis.[65] If

oxidized, LDL-cholesterol can become misconstrued as an antigen and induce an immune response.[65] Atherosclerosis compounds the microvascular distress synergistically inflicted by AGEs and PKC.

Collectively, hyperglycemia drives neurons to the point of metabolic exhaustion. As the neurons operate at maximum capacity, primary and contingent metabolic routes saturate, coenzyme stockpiles quickly deplete, and antioxidant and DNA repair mechanisms fail. These conditions disrupt intra-/intercellular communications, enable the accumulation of highly toxic ROS and RNS that damage cellular components (*e.g.* protein, DNA, synaptic vesicles, organelles), and allows for abnormal post-translational modifications (*O*-GlcNAc and AGEs) that alter cellular trafficking, signal transduction, cell morphology, and protein function/expression. This neuronal meltdown, in conjunction with the extrinsic pressures of ischemia and inflammation, drives the neuron into a degenerative state, activating the intrinsic apoptotic pathway. As neuronal viability diminishes, overall innervation and control of peripheral tissues begins to decrease, producing increasingly severe physiological effects. These physiological effects, or symptoms, are described below.

III. SYMPTOMOLOGY

Diabetic peripheral neuropathy gives rise to a variety of positive, negative, and autonomic symptoms. Positive symptoms entail spontaneous or heightened pain sensitivity, such as prickling, tingling, "pins and needles," burning, freezing, crawling, itching, throbbing, constricting, or numbness.[9, 11, 17, 66-67] Abnormal pain sensations in response to thermal and mechanical stimuli (*e.g.* brush of bed covers, walking) can

significantly alter one's quality of life.[9, 11, 17, 66-67] As the patient attempts to avoid aggravation of these hyperalgesic events, the individual can suffer from insomnia or become improperly balanced (physically), increasing the likelihood of physical injury. Imbalance can also result through the onset of negative symptoms: numbness, sensory and motor deficits, fatigue, and on rare occasions, visual impairments.[9, 11, 17, 66-67] These debilitating conditions, combined with poor circulation, promote the development of foot ulcerations and infections (*i.e.* gangrene), eventually requiring amputation. Diabetic neuropathy is the number one cause of non-traumatic, lower limb amputations in the U.S., averaging 82,000 each year.[3, 5, 66] Nerve dysfunction and poor vascular support also compromise the control and structural integrity of the autonomic nervous system. The autonomic neuropathies can provoke profuse sweating or dry skin; cardiac dysfunction (arrhythmia, infarction); gastrointestinal irregularities (constipation, diarrhea, heartburn, difficulty swallowing, nausea, and vomiting); loss of bladder sensitivity; erectile dysfunction; irregular pupil constriction/dilation; and a variety of metabolic abnormalities impacting the visceral organs (*e.g.* nephropathy).[17, 67]

Although there are several symptoms associated with diabetic peripheral neuropathy, this research focuses primarily upon the treatment of sensorimotor deficits observed in type 1 diabetic (murine) models. As previously stated, hyperglycemia drives neurons into an apoptotic state, generating an assortment of clinical symptoms as the disease progresses. Current therapeutics rely heavily upon monosymptomatic relief, addressing only portions of the underlying mechanisms driving

neurodegeneration. Several of the current therapeutic options are discussed below. However, a broader, multisymptomatic approach is needed to adequately combat diabetic neuropathy.

IV. THERAPEUTIC DEVELOPMENT

Although the Ebers Papyrus arguably describes the first reported symptoms of diabetes mellitus nearly 3500 years ago, the first indisputable account and recorded treatment were by the ancient Greek physician Aretaeus (ca. 81-138 A.D.).[16, 68-71] Aretaeus first coined the term "diabetes" from the Greek word *diabaínein*, meaning siphon or pipe-like, after making the following observations:

> Diabetes is . . . a melting down of the flesh and limbs into urine . . . life is disgusting and painful; thirst, unquenchable; excessive drinking, which, however, is disproportionate to the large quantity of urine, for more urine is passed; and one cannot stop them either from drinking or making water.[68]
>
> - Aretaeus, the Cappadocian

By 1920, the best remedies of the time remained purgation and extreme dieting, therapies employed by Aretaeus.[68-69] Individuals suffering from Type 1 diabetes, such as "J.L." (Figure 1.4.A.), usually died within a year of diagnosis as a result of malnutrition from fasting or other complications.[69, 72] The discovery and isolation of insulin by Banting, McCleod, Best, and Collip in 1922 marked the first significant therapeutic means to combat diabetes.[19, 69] With the discovery of insulin, diabetics saw not only a vast physical improvement (Figure 1.4.B.), but an increase in the average life expectancy as well.

A.  B. 

Figure 1.4. "J.L." (A) before insulin treatment, *December 15, 1922 – Age: 3 years, Weight: 15 lbs*; and (B) after insulin treatment, *February 15, 1923 – Age: 3 years, Weight 29 lbs.*[69]

While the discovery of insulin was a major stride towards treating diabetes, the global impact of diabetic complications is still evident today (see section I). In his Nobel lecture, Dr. Banting described their discovery as: "Insulin is not a cure for diabetes; it is a treatment."[73] The DCCT demonstrated that controlled, multi-daily insulin administration, in conjunction with glucose monitoring, significantly delayed further development of neuropathy, nephropathy, and retinopathy.[18] Despite insulin's prominent use in today's society, it has its drawbacks. Improper insulin management can result in diabetic hypoglycemia (insulin shock) that can cause severe brain damage or in the hyperglycemic development of potentially fatal conditions, such as diabetic ketoacidosis (increase in blood acidity due to abnormal ketone body concentrations) or diabetic coma.[61-62]

Modern diabetic treatments generally offer monosymptomatic relief or specifically inhibit single, putative pathogenic mechanisms associated with a targeted complication. Table 1.1 outlines several of the current therapeutic options available and their physiological impacts.

Table 1.1. Current therapeutic approaches to treat diabetic peripheral neuropathy.[8-17]

Neuropathic Therapies	Physiological Impact	Examples
Hormones		
Insulin (human and animal)	↑ GLUT-4 glucose transport	Rapid-, intermediate-, and slow-acting insulin preparations Continuous subcutaneous insulin infusion (CSII) therapy
Insulinmimetics	↑ GLUT-4 glucose transport	L-783,281
Hypoglycemic Agents		
Sulfonylureas, 1st and 2nd generation	↑ Insulin secretion in β-cells	Tolbutamide, Glyburide
Sulfonylureas, 3rd generation	↑ GLUT-4 glucose transport	Glimepiride
Biguanides	↓ Gluconeogenesis	Metformin
Thiazolidinediones	↑ Insulin efficacy	Rosaglitazone, Pioglitazone
α-glucosidase inhibitors	↓ glucose absorption in gut	Miglitol
Analgesics		
Opioids	↓ Pain	Tramadol, Oxycodone CR
NSAIDs	↓ Inflammation and pain	Aspirin, Ibuprofen
Additional Pain Treatments		
SSRIs	↓ Pain and depression	Paroxetine, Citalopram
SSNRIs	↓ Pain	Duloxetine, Venlafaxine
TCAs	↓ Pain and depression	Amitriptyline, Imipramine
Anticonvulsants	↓ Pain	Lamotrigine, Sodium valproate, Pregabalin
Topical	↓ Pain (localized)	Isosorbide dinitrate spray, capsaicin
Antipathogenic		
Aldose Reductase Inhibitors	↓ Sorbitol and NADPH depletion	Fidarestat, Ranirestat, Epalrestat
PKC-β Inhibitors	↓ Ischemia	Ruboxistaurin mesylate
PARP Inhibitors	↓ NAD^+ depletion	GPI-15427
Antioxidants	↓ ROS and RNS	Lycopene, α-lipoic acid, Taurine
ACE inhibitors	↓ Hypertension	Enalapril
Antiarrhytmatics	↑ Heart beat regulation	Mexilitene
Surgical		
Nerve decompression	↓ Pain or numbness	Entrapment decompression
Amputation	↓ Necrotic/infected tissues	Lower limb removal

As with insulin, several of the current therapeutics are tailored towards reestablishing homeostatic glycemic levels through insulinmimetics or hypoglycemic agents that regulate glucose absorption, transport, or production (gluconeogenesis). However, all of these options retain the hazards associated with improper insulin management. Assorted analgesics offer temporary pain relief and reduce inflammation (*i.e.* NSAIDs, non-steroidal anti-inflammatory drugs) at affected nerves. TCAs (tricyclic antidepressants) and SSRIs (selective serotonin reuptake inhibitors)

are also commonly prescribed for pain. Surgical procedures, such as limb amputation, nerve decompression, and pancreatic transplantation, are costly and accrue additional safety risks to the patient. Antirrthymatics, antihypertensive agents such as ACE (angiotensin-converting enzyme) inhibitors, and PKC-β inhibitors help to regulate and sustain adequate blood supply to the nerves. Aldose reductase inhibitors, such as Ranirestat, reduce the flux of glucose through the polyol pathway and subsequent sorbitol production. Finally, the mere increase in antioxidants helps to neutralize ROS/RNS before they can induce their cytotoxic effects.

Currently, all 54 open clinical trials dedicated towards the treatment of diabetic peripheral neuropathy are symptomatic treatments (anesthetics, anticonvulsants, hypoglycemic agents, gastrointestinal tract agents, anxiolytics, or antidepressants).[12] These approaches only slow the progression of the neuropathy. Hence, what is truly needed is a more multifaceted approach that refortifies neuronal defenses against invading glucose. This reinforcing support may be available through the upregulation of molecular chaperones known as heat shock proteins.

V. Heat Shock Proteins and Neuroprotection

Heat shock proteins (HSPs) are molecular chaperones that assist in the proper folding of nascent polypeptides, or "client proteins," into the proper conformation necessary to conduct normal physiological processes.[74-77] These chaperones also assist in the refolding of denatured proteins that might arise due to various cellular stressors, such as oxidative or nitrosative stress, nutrient deprivation, heat shock, pH fluctuations, and various pharmaceutical and toxic insults to the system.[74-75, 77]

Several of these client proteins are various oncogenic proteins that are upregulated in cancerous tissue, making heat shock proteins (esp. Hsp90) very attractive targets towards the development of novel cancer chemotherapeutics.[51, 76, 78-82] Increasing the expression of heat shock proteins, such as Hsp90, directly influences all six hallmarks of cancer (Table 1.2).[51, 79, 83]

Table 1.2. The six hallmarks of cancer.[51, 79]

Hallmark	Hsp90 Client Proteins
Self-sufficient growth signals	Raf-1, Akt, Her2, MEK, Bcr-Abl
Insensitive to anti-growth signals	Plk, Wee1, Myt1, CDK4, CDK6
Evasion of apoptosis	RIP, Akt, mutant p53, c-Met, Apaf-1, Survivin
Limitless replicative potential	Telomerase (h-Tert)
Sustained angiogenesis	FAK, Akt, Hif-1α, VEGF-R, Flt-3
Tissue invasion and metastasis	c-Met, v-src

Heat shock proteins allow cancer cells to manufacture and repair large quantities of protein, sustaining their operation under abnormal intracellular conditions (self-imposed) and encountered external stressors (*e.g.* metastasis, immune response).[51, 76, 80-81] Hence, heat shock proteins enhance viability. In contrast, the etiologies of several neurological disorders link directly to malfunctions in heat shock protein folding/refolding activity, where misfolded proteins (and their aggregates) induce cytotoxicity.[84] Heat shock proteins serve as an intracellular quality assurance/quality control: triaging proteins for either repair or flagging them for proteolytic degradation via ubiquitination, disaggregating aberrant protein complexes, stabilizing critical protein complexes, and trafficking proteins to their proper destinations. Table 1.3 depicts several neurodegenerative diseases that arise as the result of altered (*e.g.* client protein mutation) or insufficient HSP:client protein interactions.

Table 1.3. Neurological disorders associated with HSP deficiencies.[84-96]

Disease	Protein
Alzheimer's Disease	Amyloid-β, hyperphosphorylated tau
Parkinson's Disease	α-synuclein
Amyotrophic Lateral Sclerosis (ALS or Lou Gehrig's Disease),	Mutant superoxide dismutase-1 (SOD1)
Retinitis Pigmentosa	Mutant rhodopsin
Huntington's Disease	Mutant huntingtIn (mtt)
Spinocerebellar Ataxias (SCA) Types: 1, 2, 3, 6, 7, 12, and 17	Mutant ataxins
Spinal and Bulbar Muscular Atrophy (SBMA or Kennedy's Disease)	Mutant androgen receptor
Dentatorupallidolysian Atrophy (DRPLA)	Mutant atrophin-1
Creutzfeldt–Jakob Disease	PrP^{C}/PrP^{Sc}

Upregulation of heat shock proteins not only reduces the formation of these abnormal proteins, but solubilizes and disbands their toxic aggregates.[84, 87, 90-91, 95] As previously mentioned, diabetes-induced hyperglycemic stress damages or alters the expression and functional integrity of several proteins and transcription factors. HSP client proteins are involved in numerous cellular operations that directly/indirectly impact neuronal survival (Table 1.4).

Table 1.4. Heat shock protein associations affecting neuronal viability.

Neuroprotective Attributes	Hsp90, Hsp70, & HSR-Associated Proteins
Mitochondrial regulation	Mn/Cu SOD, HO-1, NOS (all isoforms), Hsp60, TOM70
Unfolded Protein Response (UPR)	Grp94, Grp78, Calreticulin, IRE-1α, Perk
Evasion of apoptosis	Akt, Apaf-1, Bcl-XL, Survivin
Transcription/Translation Regulation	Raf-1, MEK, ERK, Akt, mTOR, GSK-3β, JAK, PARP
Insulin signaling	IR, IGF-R, Akt
Vesicle maintenance	Hsp40, Neural J Proteins, Hsc70
Demyelination inhibition	JNK, PrP^{C}
Vascular support	Akt, Hif-1α, VEGF-R

Thus, under hyperglycemic stress, heat shock proteins offer a potential mechanism to salvage damaged proteins, stabilize essential protein-protein interactions, sequester proteins that advocate apoptosis, and facilitate the folding and delivery of reinforcing protein support. The majority of heat shock proteins can be upregulated through the induction of the heat shock response.

Hsp90 and the Heat Shock Response

Hsp90 is a 90-kDa molecular chaperone that comprises 1-2% of all cellular proteins and interacts with over 200 client proteins and 50 co-chaperones.[51, 76-81, 83] There are four mammalian isoforms: Hsp90α and Hsp90β (cytosol), Grp94 (glucose-regulated protein-94) (endoplasmic reticulum), and TRAP-1 (tumor necrosis factor receptor associated protein-1) (mitochondria). As mentioned previously, small molecular inhibitors of Hsp90 can induce cytotoxicity in cancer cells by preventing sufficient protein folding needed to sustain accelerated cancerous activities (Figure 1.5).[51, 74-83, 97] Hsp90 also constitutively binds heat shock factor-1 (HSF-1), a transcription factor that induces the pro-survival heat shock response (HSR).[98-99]

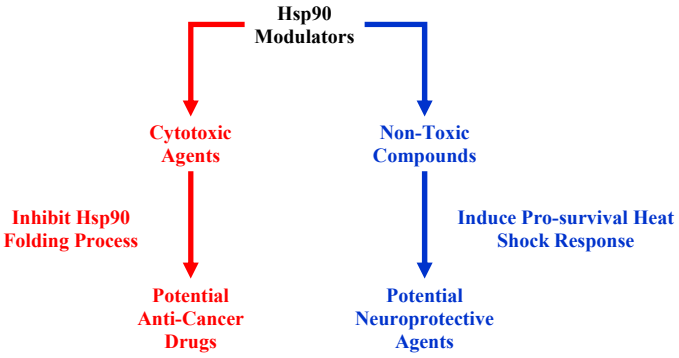

Figure 1.5. Cytotoxic versus neuroprotective roles of Hsp90 modulators.[79]

Upon heat shock or inhibition of Hsp90 (homodimer), HSF-1 releases, phosphorylates, trimerizes, hyperphosphorylates, and translocates into the nucleus, wherein it binds to a series of heat shock elements (HSEs) (Figure 1.6).[83, 98, 100] This allows for the transcription and expression of additional heat shock proteins, such as Hsp72 (inducible Hsp70), Hsp40, Hsp27, and additional Hsp90.

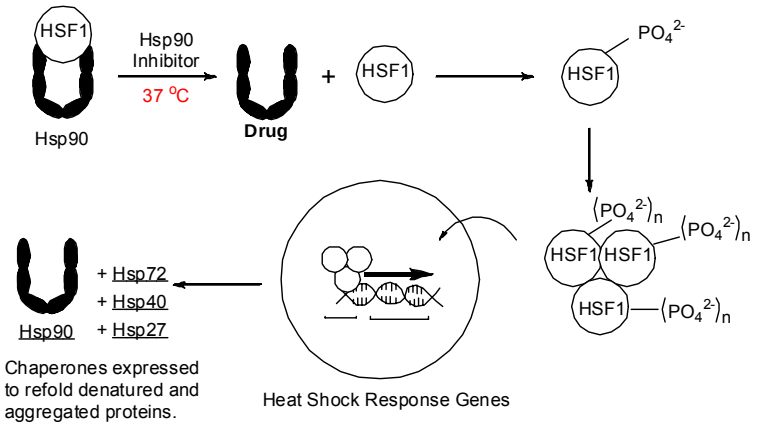

Figure 1.6. Induction of the heat shock response via HSF-1 release from Hsp90.[79]

Current Hsp90 inhibitors are therapeutically problematic. *N*-terminal inhibitors, such as the benzoquinone ansamycin antibiotic geldanamycin, induce immediate client protein degradation while simultaneously inducing the heat shock response via HSF-1 release (Figure 1.7).[101] *C*-terminal inhibitors, such as the coumarin antibiotic novobiocin and structural analog KU-174, induce immediate client protein degradation with little to no induction of the HSR.[97] However, through the optimization and characterization of the novobiocin scaffold, a unique structural analog, KU-32, was created. KU-32 delays the onset of Hsp90 client protein degradation in a dose-dependent manner while promptly inducing the HSR.[102] Hence, KU-32 appears to act more as a modulator of Hsp90 activity versus an inhibitor. This generates a novel therapeutic window in which to operate in and offer neuroprotection.

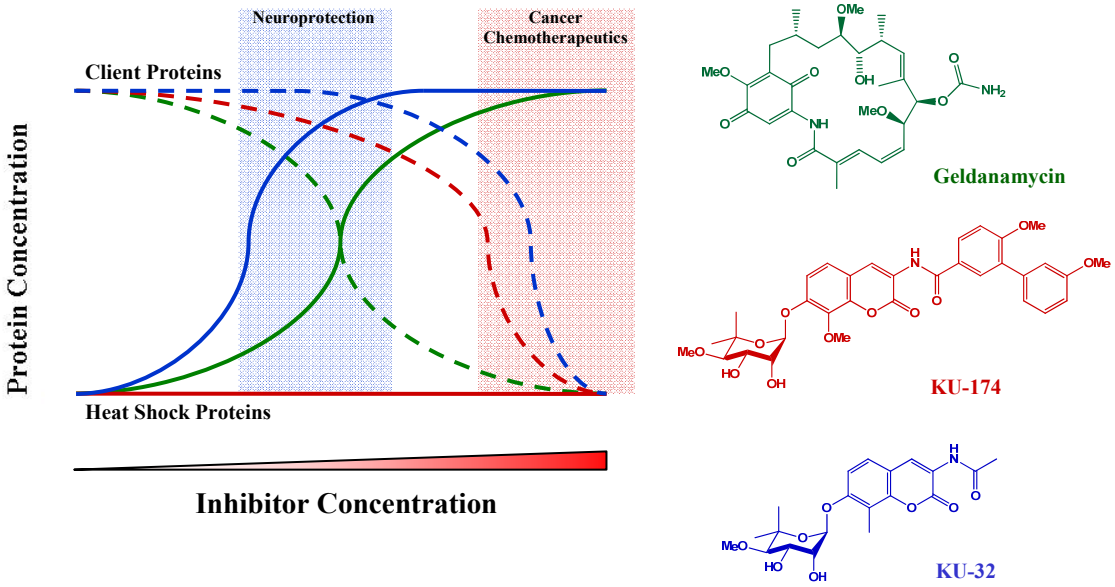

Figure 1.7. Client protein degradation and induction of the heat shock response with the three known types of Hsp90 inhibitors.[75]

Hsp90 works collaboratively with several co-chaperones, partner proteins, and immunophilins to form stabilized heteroprotein complexes in which it operates upon client proteins. In addition to assisting in Hsp90 client protein folding, Hsp70 and Hsp40, also upregulated during the HSR, can form separate complexes capable of offering additional neuroprotective roles. These functions are discussed briefly below.

Hsp70 and Hsp40

Although there are ~13 Hsp70 isoforms, the primary focus of this section is on constitutive Hsc70 (heat shock cognate 70) and the inducible isoforms: Hsp72 (humans) and Hsp70.1/Hsp70.3 (mice).[103-104] There are over 40 different mammalian proteins that contain a signature J domain (known as "J proteins"), including Hsp40. The J domain enables these proteins to bind to Hsp70 and catalyze Hsp70's ATPase activity.[103-104] There are a multitude of combinations in which J proteins can complex

with Hsp70, altering substrate recognition and increasing the number of potential client proteins.[103] Neurons employ several specialized Hsp70:J protein interactions to accomplish essential neuronal functions and prevent neurodegeneration (Table 1.5).[104]

Table 1.5. Hsp70 interactions with neural J proteins.[104-106]

J Protein	Function	Location
Auxilin	Clathrin exchange during endocytosis of vesicles	Cytosol
GAK (Cyclin G-associated kinase)	Clathrin exchange during endocytosis of vesicles	Cytosol
CSPα (Cysteine string protein α)	$G_{\alpha s}$ GEF (guanine nucleotide exchange factor) Ca^{2+} channel regulation Exocytosis-associated protein repair (SNARE)	Synaptic vesicles
Rme-8	Endosomal trafficking regulation	Endosome
Hsp40	Refolding damaged proteins	Cytosol
Hsj1	Sorting of polyubiquitylated proteins for degradation	Cytosol/ER
Mrj	Solubilization of cytotoxic aggregates	Cytosol/Nucleus
Rdj2	$G_{\alpha s}$ GEF PrP^C	Cytosol/Membrane

Several neural J proteins show interchangeability between Hsc70 and inducible Hsp70 and *vice versa*.[104-105] However, this interplay is often accompanied by differences in relative binding affinities. Specialized Hsp70:neural J protein complexes assist in synaptic vesicle management (*e.g.* calcium channel regulation, exocytosis, endocytosis), serve as GEFs (guanine nucleotide exchange factors) to stimulate $G_{\alpha s}$ in G-protein coupled receptors (GPCRs), and assist in protein ubiquitination. Through interactions with BAG-1 (BCL2-associated athanogene) and CHIP (*C*-terminus of Hsc70/Hsp70-interacting protein), Hsp70/Hsc70 flags irreparable proteins with ubiquitin.[107] This enables the degradation of both Hsp90 and Hsp70 client proteins.

Hsp70 and Hsc70 also display lectin properties (*i.e.* binds *O*-GlcNAc-proteins) that enable them to bind *O*-GlcNAcylated proteins (see hexosamine pathway), including several heat shock proteins (Hsp70, Hsc70, Hsp90, Hsp60, and Hsp27).[44-45, 50, 108-113] It's currently hypothesized that Hsp70/Hsc70 employs these properties to

protect proteins from degradation.[108-109] Thus, induction of Hsp70 could additionally serve as a means to sequester and protect critical proteins and other chaperones (*i.e.* Hsp60) within the neuron. However, the impact of *O*-GlcNAc on heat shock protein expression and function and substrate recognition is poorly understood.

Preliminary Data and Hypothesis

Induction of the heat shock response may reinforce fatigued neurons by clearing irreparable proteins, refolding damaged proteins, transporting proteins to areas of concern, sequestering and protecting essential proteins from degradation, and stabilizing protein complexes. Several of these inducible heat shock proteins (Hsp90, Hsp70, and Hsp40) are localized within dysfunctional organelles and associate directly with pathways implicated in glucose neurotoxicity.

Based on these premises, a preliminary study of the *in vitro* neuroprotective effects of KU-32 in SC-DRG (Schwann cell-dorsal root ganglia) co-cultures was undertaken. Neuregulin-1 type II (NRG-1) specifically binds to Erb-B2/B3 receptors in Schwann cells and induces demyelinating hypertrophic neuropathy.[114-117] Thus, the hypothesis was tested as to whether the prophylactic treatment of KU-32 would reduce the degree of NRG-1-induced demyelination of the SC-DRG co-cultures. SC-DRG co-cultures were established, dosed with 0, 0.1, or 1 μM KU-32 for 2 hours, and subsequently administered 0 or 100 ng/ml NRG-1.[116] All co-cultures were immunostained for myelin basic protein (red) and imaged using fluorescence microscopy (Figure 1.8). KU-32 treatment of the co-cultures in the absence of NRG-1 displayed no morphological changes. Administration of NRG-1 reduced myelination

by ~25%, as indicated by reduced segment length and increased vesiculation. However, the pretreatment with KU-32 revealed a dose-dependent negation in demyelination.

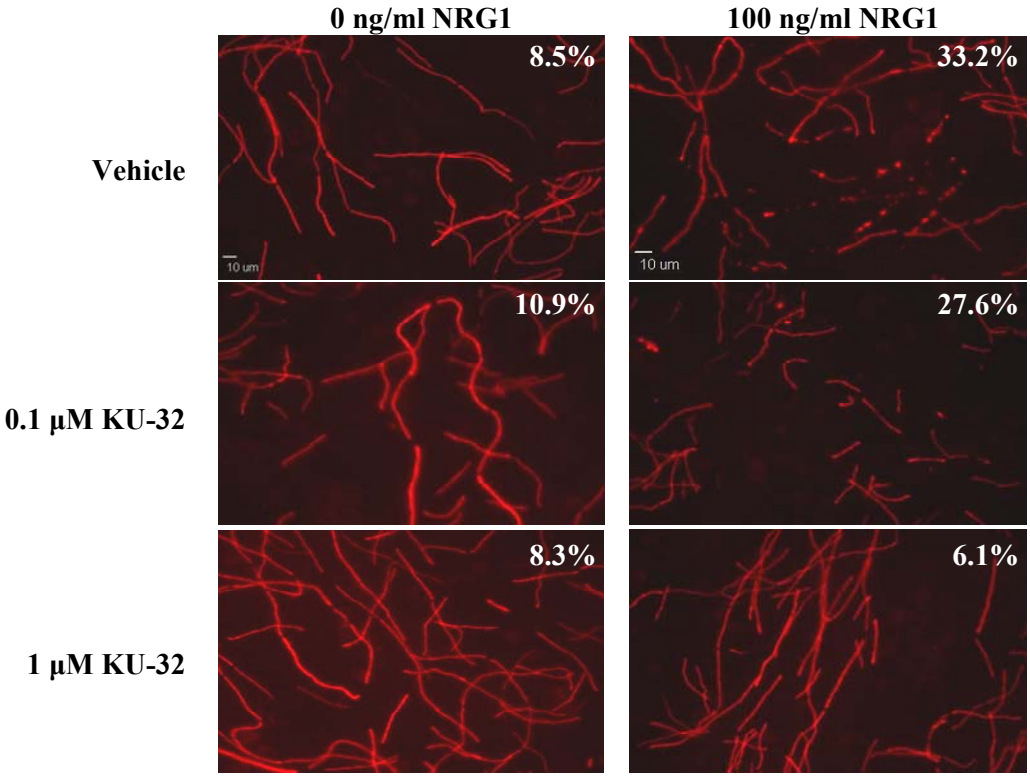

Figure 1.8. Pretreatment with KU-32 prevents NRG1-induced demyelination in dose dependent manner. Myelinated SC-DRG co-cultures were pre-treated with the indicated concentrations of KU-32 for 2 hrs prior to the addition of 100 ng/ml NRG1. After 48 hrs, the cells were immunostained for myelin basic protein (red) and imaged using fluorescence microscopy. The extent of damaged myelin segments (decrease in fluorescence) was expressed relative control untreated co-cultures (% damage indicated in each panel relative). KU-32 alone does not alter segment morphology but prevents the shortening and vesiculation of the segments.

In addition, the potential abilities of KU-32 to protect against hyperglycemic stress were also assessed in unmyelinated primary sensory neurons. Embryonic DRGs were pretreated with 0.1-1 µM KU-32 for 24 hours in 25 mM glucose media (low glucose, LG) and then raised to 45 mM glucose (high glucose, HG) for an additional

24 hours (Figure 1.9). Assessment of cell viability revealed that hyperglycemia induced ~1.5-fold increase in DRG death. This was negated with both KU-32 treatments.

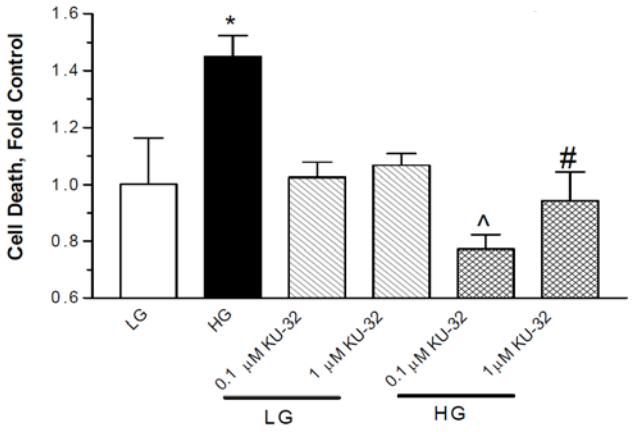

Figure 1.9. KU-32 protects sensory neurons against glucose-induced death. After 24 hours of pretreatment with 0.1-1 μM KU-32 in 25 mM glucose media (low glucose, LG), glucose concentrations were raised to 45 mM glucose (high glucose, HG) for an additional 24 hours in DRG cultures. Cell viability was assessed and expressed as fold control. Hyperglycemia induced ~1.5-fold increase in DRG death, which was negated via KU-32 treatment.* $p < 0.05$ versus LG control; ^, $p < 0.003$ versus HG; #, $p<0.02$ versus HG (n=3).

Since KU-32 protected these *in vitro* models of myelinated and unmyelinated nerves, we examined whether the induction of the heat shock response through Hsp90 modulation could decrease or reverse the pathophysiological progression of DPN in Type-1 diabetic mice. We hypothesized that a small molecule modulator of Hsp90 will improve experimental diabetic neuropathy

VI. References

1. International Diabetes Federation. IDF Diabetes Atlas 2009. http://www.diabetesatlas.org/.

2. United Nations General Assembly, A/RES/61/225. World Diabetes Day. Nations, U., Ed. United Nations: New York, 2007; p 2.

3. American Diabetes Association, *Diabetes Care* **2008,** *31* (3), 596-615.

4. American Diabetes Association. Diabetes. 2010. http://www.diabetes.org/.

5. Centers for Disease Control and Prevention, National diabetes fact sheet: general information and national estimates on diabetes in the United States, 2007. Department of Health and Human Services, Centers for Disease Control and Prevention: Atlanta, GA, 2008.

6. World Health Organization. Fact Sheet N°312: Diabetes 2009. http://www.who.int/mediacentre/factsheets/fs312/en/.

7. CDC's Division of Diabetes Translation. National Diabetes Surveillance System. 2009. http://www.cdc.gov/diabetes/statistics.

8. Boulton, A. J., *Curr Opin Endocrinol Diabetes Obes* **2007,** *14* (2), 141-5.

9. Boulton, A. J.; Malik, R. A.; Arezzo, J. C.; Sosenko, J. M., *Diabetes Care* **2004,** *27* (6), 1458-86.

10. Goodman, L. S.; Hardman, J. G.; Limbird, L. E.; Gilman, A. G., *Goodman & Gilman's the pharmacological basis of therapeutics*. 10th ed.; McGraw-Hill, Medical Pub. Division: New York, 2001; p xxvii, 2148 p.

11. Mahmood, D.; Singh, B. K.; Akhtar, M., *J Pharm Pharmacol* **2009,** *61* (9), 1137-45.

12. National Institutes of Health. ClinicalTrials.gov 2010. http://www.clinicaltrials.gov/ct2/home.

13. Obrosova, I. G., *Neurotherapeutics* **2009,** *6* (4), 638-47.

14. Obrosova, I. G.; Julius, U. A., *Curr Vasc Pharmacol* **2005,** *3* (3), 267-83.

15. Vinik, A.; Ullal, J.; Parson, H. K.; Casellini, C. M., *Nat Clin Pract Endocrinol Metab* **2006,** *2* (5), 269-81.

16. Williams, D. A.; Lemke, T. L., *Foye's principles of medicinal chemistry*. 5th ed.; Lippincott Williams & Wilkins: Philadelphia, 2002; p xii, 1114 p.

17. Zochodne, D. W., *Muscle Nerve* **2007,** *36* (2), 144-66.

18. *N Engl J Med* **1993,** *329* (14), 977-86.

19. Banting, F. G.; Best, C. H., *Pancreatic extracts in the treatment of diabetes mellitus : preliminary report*. s.n.: [S.l., p 6 p.

20. Minkowski, O., *Diabetes* **1989,** *38* (1), 1-6.

21. Crofford, O. B.; Minemura, T.; Kono, T., *Adv Enzyme Regul* **1970,** *8*, 219-38.

22. Freychet, P.; Roth, J.; Neville, D. M., Jr., *Proc Natl Acad Sci U S A* **1971,** *68* (8), 1833-7.

23. Renner, R., *FEBS Lett* **1973,** *32* (1), 87-90.

24. Kern, M.; Wells, J. A.; Stephens, J. M.; Elton, C. W.; Friedman, J. E.; Tapscott, E. B.; Pekala, P. H.; Dohm, G. L., *Biochem J* **1990,** *270* (2), 397-400.

25. Tomlinson, D. R.; Gardiner, N. J., *Nat Rev Neurosci* **2008,** *9* (1), 36-45.

26. Muona, P.; Sollberg, S.; Peltonen, J.; Uitto, J., *Diabetes* **1992,** *41* (12), 1587-96.

27. Gerhart, D. Z.; Broderius, M. A.; Borson, N. D.; Drewes, L. R., *Proc Natl Acad Sci U S A* **1992,** *89* (2), 733-7.

28. Bell, G. I.; Kayano, T.; Buse, J. B.; Burant, C. F.; Takeda, J.; Lin, D.; Fukumoto, H.; Seino, S., *Diabetes Care* **1990,** *13* (3), 198-208.

29. Magnani, P.; Cherian, P. V.; Gould, G. W.; Greene, D. A.; Sima, A. A.; Brosius, F. C., 3rd, *Metabolism* **1996,** *45* (12), 1466-73.

30. Wang, Z.; Gleichmann, H., *Diabetes* **1998,** *47* (1), 50-6.

31. Guthrie, R. A.; Guthrie, D. W., *Crit Care Nurs Q* **2004,** *27* (2), 113-25.

32. American Diabetes Association, *Diabetes Care* **2003,** *26 Suppl 1*, S5-20.

33. Kyvik, K. O.; Green, A.; Beck-Nielsen, H., *BMJ* **1995,** *311* (7010), 913-7.

34. Condon, J.; Shaw, J. E.; Luciano, M.; Kyvik, K. O.; Martin, N. G.; Duffy, D. L., *Twin Res Hum Genet* **2008,** *11* (1), 28-40.

35. Hyttinen, V.; Kaprio, J.; Kinnunen, L.; Koskenvuo, M.; Tuomilehto, J., *Diabetes* **2003,** *52* (4), 1052-5.

36. Redondo, M. J.; Yu, L.; Hawa, M.; Mackenzie, T.; Pyke, D. A.; Eisenbarth, G. S.; Leslie, R. D., *Diabetologia* **2001,** *44* (3), 354-62.

37. O'Rahilly, S., *Nature* **2009,** *462* (7271), 307-14.

38. *Diabetes Care* **1999,** *22* (4), 623-34.

39. Nelson, D. L.; Cox, M. M.; Lehninger, A. L., *Lehninger principles of biochemistry*. 4th ed.; W.H. Freeman: New York, 2005; p 1 v. (various pagings).

40. Obrosova, I. G., *Biochim Biophys Acta* **2009,** *1792* (10), 931-40.

41. Figueroa-Romero, C.; Sadidi, M.; Feldman, E. L., *Rev Endocr Metab Disord* **2008,** *9* (4), 301-14.

42. Arner, R. J.; Prabhu, K. S.; Krishnan, V.; Johnson, M. C.; Reddy, C. C., *Biochem Biophys Res Commun* **2006,** *339* (3), 816-20.

43. ExplorEnz: The Enzyme Database UDP-N-acetylglucosamine Biosynthesis. http://www.enzyme-database.org/reaction/polysacc/UDPGlcN.html.

44. Zachara, N. E.; O'Donnell, N.; Cheung, W. D.; Mercer, J. J.; Marth, J. D.; Hart, G. W., *J Biol Chem* **2004,** *279* (29), 30133-42.

45. Butkinaree, C.; Park, K.; Hart, G. W., *Biochim Biophys Acta* **2010,** *1800* (2), 96-106.

46. Cheng, X.; Hart, G. W., *J Biol Chem* **2001,** *276* (13), 10570-5.

47. Chou, T. Y.; Hart, G. W.; Dang, C. V., *J Biol Chem* **1995,** *270* (32), 18961-5.

48. Hiromura, M.; Choi, C. H.; Sabourin, N. A.; Jones, H.; Bachvarov, D.; Usheva, A., *J Biol Chem* **2003,** *278* (16), 14046-52.

49. Fiordaliso, F.; Leri, A.; Cesselli, D.; Limana, F.; Safai, B.; Nadal-Ginard, B.; Anversa, P.; Kajstura, J., *Diabetes* **2001,** *50* (10), 2363-75.

50. Hu, P.; Shimoji, S.; Hart, G. W., *FEBS Lett* **2010,** *584* (12), 2526-2538.

51. Weinberg, R. A., *The biology of cancer*. Garland Science: New York, NY, 2007; p 1 v. (various pagings).

52. Amadori, M., *Atti. accad. Lincci* **1925,** *6* (2), 337-342.

53. Kürti, L.; Czakó, B., *Strategic applications of named reactions in organic synthesis : background and detailed mechanisms*. Elsevier Academic Press: Amsterdam ; Boston, 2005; p lii, 758 p.

54. Glenn, J. V.; Stitt, A. W., *Biochim Biophys Acta* **2009,** *1790* (10), 1109-16.

55. Sugimoto, K.; Yasujima, M.; Yagihashi, S., *Curr Pharm Des* **2008,** *14* (10), 953-61.

56. Vincent, A. M.; Perrone, L.; Sullivan, K. A.; Backus, C.; Sastry, A. M.; Lastoskie, C.; Feldman, E. L., *Endocrinology* **2007,** *148* (2), 548-58.

57. Mohamed, A. K.; Bierhaus, A.; Schiekofer, S.; Tritschler, H.; Ziegler, R.; Nawroth, P. P., *Biofactors* **1999,** *10* (2-3), 157-67.

58. American Diabetes Association, *Diabetes Care* **2010,** *33 Suppl 1*, S4-10.

59. Geraldes, P.; King, G. L., *Circ Res* **2010,** *106* (8), 1319-31.

60. Cameron, N. E.; Cotter, M. A., *Diabetes Metab Res Rev* **2002,** *18* (4), 315-23.

61. Laffel, L., *Diabetes Metab Res Rev* **1999,** *15* (6), 412-26.

62. Brenner, Z. R., *AACN Clin Issues* **2006,** *17* (1), 56-65; quiz 91-3.

63. Wiggin, T. D.; Sullivan, K. A.; Pop-Busui, R.; Amato, A.; Sima, A. A.; Feldman, E. L., *Diabetes* **2009,** *58* (7), 1634-40.

64. Fagot-Campagna, A.; Rolka, D. B.; Beckles, G. L.; Gregg, E. W.; Narayan, K. M., *Diabetes* **2000,** *49* (5), A78.

65. Dokken, B. B., *Diabetes Spectrum* **2008,** *21* (3), 160-165.

66. Cheer, K.; Shearman, C.; Jude, E. B., *BMJ* **2009,** *339*, b4905.

67. Vinik, A. I.; Freeman, R.; Erbas, T., *Semin Neurol* **2003,** *23* (4), 365-72.

68. Aretaeus; Adams, F.; Banov, L., *Aretaiou Kappadokou ta sozomena = The extant works of Aretaeus, the Cappadocian*. Milford House: Boston, 1972; p xx, 510 p.

69. Bliss, M., *The discovery of insulin*. University of Chicago Press: Chicago, 1982; p 304 p., [16] p. of plates.

70. Engelhardt, D. v., *Diabetes, its medical and cultural history : outlines, texts, bibliography*. Springer-Verlag: Berlin ; New York, 1989; p x, 491 p.

71. Loriaux, D. L., *The Endocrinologist* **2006,** *16* (2), 55-56.

72. Bliss, M., *Horm Res* **2005,** *64 Suppl 2*, 98-102.

73. Banting, F. G., Nobel Lecture: Diabetes and Insulin. The Nobel Foundation: Stockholm, Sweden, 1923.

74. Peterson, L. B.; Blagg, B. S., *Future Med Chem* **2009,** *1* (2), 267-283.

75. Amolins, M. W.; Blagg, B. S., *Mini Rev Med Chem* **2009,** *9* (2), 140-52.

76. Pearl, L. H.; Prodromou, C.; Workman, P., *Biochem J* **2008,** *410* (3), 439-53.

77. Chaudhury, S.; Welch, T. R.; Blagg, B. S., *ChemMedChem* **2006,** *1* (12), 1331-40.

78. Picard, D. Hsp90 Interactors. 2010. www.picard.ch/downloads/Hsp90interactors.pdf (accessed June 2010).

79. Donnelly, A.; Blagg, B. S., *Curr Med Chem* **2008,** *15* (26), 2702-17.

80. Whitesell, L.; Lindquist, S. L., *Nat Rev Cancer* **2005,** *5* (10), 761-72.

81. Pratt, W. B.; Toft, D. O., *Exp Biol Med (Maywood)* **2003,** *228* (2), 111-33.

82. Taldone, T.; Chiosis, G., *Curr Top Med Chem* **2009,** *9* (15), 1436-46.

83. Neckers, L., *J Biosci* **2007,** *32* (3), 517-30.

84. Muchowski, P. J.; Wacker, J. L., *Nat Rev Neurosci* **2005,** *6* (1), 11-22.

85. Bandopadhyay, R.; de Belleroche, J., *Trends Mol Med* **2010,** *16* (1), 27-36.

86. Dou, F.; Netzer, W. J.; Tanemura, K.; Li, F.; Hartl, F. U.; Takashima, A.; Gouras, G. K.; Greengard, P.; Xu, H., *Proc Natl Acad Sci U S A* **2003,** *100* (2), 721-6.

87. Richter-Landsberg, C., *Heat shock proteins in neural cells*. Landes Bioscience ; Springer Science+Business Media: Austin, Tex.
New York, 2007; p 115 p.

88. Ansar, S.; Burlison, J. A.; Hadden, M. K.; Yu, X. M.; Desino, K. E.; Bean, J.; Neckers, L.; Audus, K. L.; Michaelis, M. L.; Blagg, B. S., *Bioorg Med Chem Lett* **2007,** *17* (7), 1984-90.

89. Lu, Y.; Ansar, S.; Michaelis, M. L.; Blagg, B. S., *Bioorg Med Chem* **2009,** *17* (4), 1709-15.

90. Asea, A. A. A.; Brown, I. R., *Heat shock proteins and the brain : implications for neurodegenerative diseases and neuroprotection*. Springer: [Dordrecht], 2008; p xvi, 373 p.

91. Brown, I. R., *Ann N Y Acad Sci* **2007,** *1113*, 147-58.

92. Hands, S. L.; Wyttenbach, A., *Acta Neuropathol* **2010**.

93. Batulan, Z.; Taylor, D. M.; Aarons, R. J.; Minotti, S.; Doroudchi, M. M.; Nalbantoglu, J.; Durham, H. D., *Neurobiol Dis* **2006,** *24* (2), 213-25.

94. Kalmar, B.; Greensmith, L., *Cell Mol Biol Lett* **2009,** *14* (2), 319-35.

95. Luo, W.; Sun, W.; Taldone, T.; Rodina, A.; Chiosis, G., *Mol Neurodegener* **2010,** *5* (1), 24.

96. Winklhofer, K. F.; Heller, U.; Reintjes, A.; Tatzelt, J., *Traffic* **2003,** *4* (5), 313-22.

97. Donnelly, A. C.; Mays, J. R.; Burlison, J. A.; Nelson, J. T.; Vielhauer, G.; Holzbeierlein, J.; Blagg, B. S., *J Org Chem* **2008,** *73* (22), 8901-20.

98. Zou, J.; Guo, Y.; Guettouche, T.; Smith, D. F.; Voellmy, R., *Cell* **1998,** *94* (4), 471-80.

99. Morange, M., *Handb Exp Pharmacol* **2006,** (172), 153-69.

100. Shamovsky, I.; Nudler, E., *Cell Mol Life Sci* **2008,** *65* (6), 855-61.

101. Whitesell, L.; Mimnaugh, E. G.; De Costa, B.; Myers, C. E.; Neckers, L. M., *Proc Natl Acad Sci U S A* **1994,** *91* (18), 8324-8.

102. Mollapour, M.; Tsutsumi, S.; Donnelly, A. C.; Beebe, K.; Tokita, M. J.; Lee, M. J.; Lee, S.; Morra, G.; Bourboulia, D.; Scroggins, B. T.; Colombo, G.; Blagg, B. S.; Panaretou, B.; Stetler-Stevenson, W. G.; Trepel, J. B.; Piper, P. W.; Prodromou, C.; Pearl, L. H.; Neckers, L., *Mol Cell* **2010,** *37* (3), 333-43.

103. Patury, S.; Miyata, Y.; Gestwicki, J. E., *Curr Top Med Chem* **2009,** *9* (15), 1337-51.

104. Zhao, X.; Braun, A. P.; Braun, J. E., *Cell Mol Life Sci* **2008,** *65* (15), 2385-96.

105. Gibbs, S. J.; Barren, B.; Beck, K. E.; Proft, J.; Zhao, X.; Noskova, T.; Braun, A. P.; Artemyev, N. O.; Braun, J. E., *PLoS One* **2009,** *4* (2), e4595.

106. Rosales-Hernandez, A.; Beck, K. E.; Zhao, X.; Braun, A. P.; Braun, J. E., *Cell Stress Chaperones* **2009,** *14* (1), 71-82.

107. Demand, J.; Alberti, S.; Patterson, C.; Hohfeld, J., *Curr Biol* **2001,** *11* (20), 1569-77.

108. Guinez, C.; Lemoine, J.; Michalski, J. C.; Lefebvre, T., *Biochem Biophys Res Commun* **2004,** *319* (1), 21-6.

109. Guinez, C.; Losfeld, M. E.; Cacan, R.; Michalski, J. C.; Lefebvre, T., *Glycobiology* **2006,** *16* (1), 22-8.

110. Lefebvre, T.; Cieniewski, C.; Lemoine, J.; Guerardel, Y.; Leroy, Y.; Zanetta, J. P.; Michalski, J. C., *Biochem J* **2001,** *360* (Pt 1), 179-88.

111. Wells, L.; Vosseller, K.; Cole, R. N.; Cronshaw, J. M.; Matunis, M. J.; Hart, G. W., *Mol Cell Proteomics* **2002,** *1* (10), 791-804.

112. Walgren, J. L.; Vincent, T. S.; Schey, K. L.; Buse, M. G., *Am J Physiol Endocrinol Metab* **2003,** *284* (2), E424-34.

113. Kim, H. S.; Kim, E. M.; Lee, J.; Yang, W. H.; Park, T. Y.; Kim, Y. M.; Cho, J. W., *FEBS Lett* **2006,** *580* (9), 2311-6.

114. Dobrowsky, R. T.; Rouen, S.; Yu, C., *J Pharmacol Exp Ther* **2005,** *313* (2), 485-91.

115. McGuire, J. F.; Rouen, S.; Siegfreid, E.; Wright, D. E.; Dobrowsky, R. T., *Diabetes* **2009,** *58* (11), 2677-86.

116. Yu, C.; Rouen, S.; Dobrowsky, R. T., *Glia* **2008,** *56* (8), 877-87.

117. Huijbregts, R. P.; Roth, K. A.; Schmidt, R. E.; Carroll, S. L., *J Neurosci* **2003,** *23* (19), 7269-80.

CHAPTER 2: MATERIALS AND METHODS

I. ANIMALS

Wild-type (WT) C57 Bl/6 mice were purchased from Harlan Laboratories (Indianapolis, IN). Hsp70.1/70.3 double knockout mice were attained from the Mutant Mouse Resource Center (San Diego, CA). All animals were maintained on a 12 hour light/dark cycle and maintained at 70°C and 70% humidity with *ad libitum* access to water and Purina diet 5001 chow. All animal procedures (*e.g.* tagging, handling, fasting, blood draw, drug administration, euthanasia, and colony management) were conducted in accordance with NIH (National Institutes of Health) regulations and protocols approved by the Institutional Animal Care and Use Committee (IACUC).

II. INDUCTION OF DIABETES

Eight-week old wild-type (WT) C57 Bl/6 mice and Hsp70.1/70.3 double knockout mice were rendered diabetic through a series of intraperitoneal (IP) injections of streptozoticin (STZ) (Sigma Aldrich, St. Louis, MO) in 200 µl sterile saline buffered solution (10 mM sodium citrate, 154 mM NaCl, pH 4.5). Streptozotocin is a nitrosourea alkyating agent that contains a glucose-moiety enabling selective transport by the GLUT-2 glucose transporters of the β-cells (Figure 2.1).[1-2] STZ methylates pancreatic β-cell DNA, inhibiting transcription and inadvertently inducing cell death.[1-2]

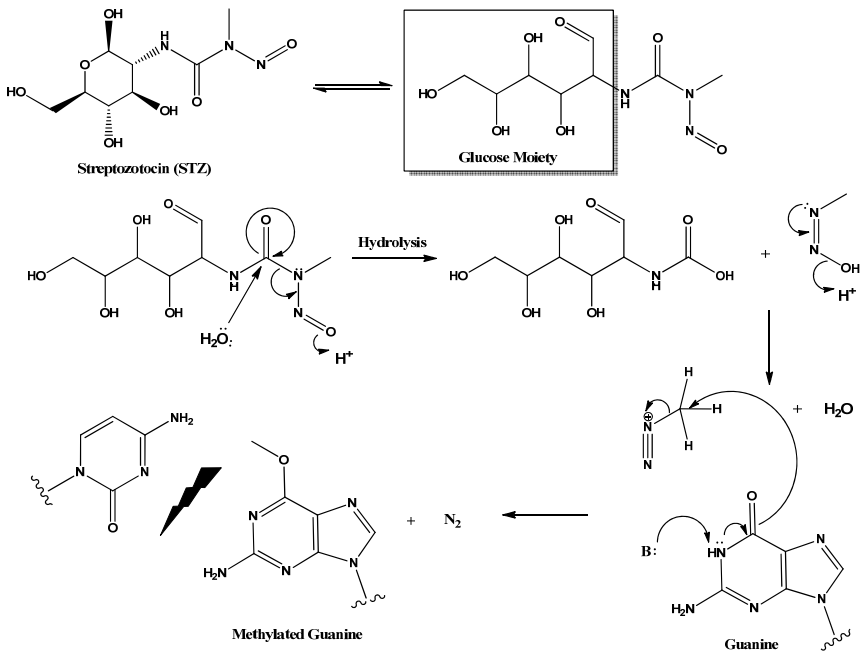

Figure 2.1. Proposed mechanism of streptozotocin-induced methylation of pancreatic β-cell DNA.

All mice were fasted overnight to minimize competitive pancreatic absorption of glucose, ensuring maximal STZ uptake. Diabetic mice received daily injections of STZ over the course of three days at 85 mg/kg (day 1), 70 mg/kg (day 2), and 55 mg/kg (day 3). Mice were fasted an additional two hours post-IP injection. Fasting plasma glucose levels were measured three days after the final STZ injection in accordance with the procedure outlined below. Mice with FBG (fasting blood glucose) levels > 290 mg/dl (16 mM) were deemed diabetic and were admitted into the study. Mice with FBG < 250 mg/dl were re-administered up to two additional STZ injections at 85 mg/kg. Only mice with FBG > 290 mg/dl were admitted into the study. Periodic reassessments of fasting plasma glucose were conducted throughout and at the conclusion of all studies to monitor maintenance of the diabetic phenotype.

Glycated hemoglobin levels (HbA_{1C}) were also measured upon study completion to validate the long-term maintenance of diabetes due to the formation of advanced glycation endproducts.

III. Fasting Plasma Glucose and Glycated Hemoglobin Measurements

Blood was drawn from tip of the tail in all mice to measure fasting plasma glucose and glycated hemoglobin (HBA_{1C}) levels. Fasting plasma glucose levels were measured using a commercial One Touch II glucose meter (Lifescan, Milpitas, CA) after a 12-hour fast. Percent glycated hemoglobin levels were measured using the A1C NOW+ multi test A1C kit (Bayer Healthcare, Sunnyvale, CA). HbA_{1C} levels $\geq$ 6.5% were deemed diabetic (comparable to humans).[1]

IV. Drug Formulation

KU-32 was synthesized in accordance with published procedures.[2] The compound was delivered intraperitoneally based upon the mass of the specimen. Due to problems with solubility, KU-32 was dissolved in 0.1 M Captisol (CyDex Pharmaceuticals, Lenexa, KS) in sterile 1X phosphate buffered saline (PBS) (137 mM NaCl, 2.7 mM KCl, 100 mM Na_2HPO_4, 2 mM KH_2PO_4, pH 7.4). 200 µl sterile 1X PBS were used per injection as a vehicle. Control mice were treated with equivalent amounts of KU-32-free 0.1 M Captisol solution and sterile 200 µl sterile 1X PBS. All injection sites were cleaned using 70% ethanol prior to an injection.

V. Assessment of Thermal Sensitivity

The Hargreaves analgesiometer (Ugo Basile, Comerio, Italy) was used to assess response to thermal stimuli.[3] Animals were placed under a 1 L glass beaker on a glass

platform and allowed to acclimate for 30-40 minutes. The Hargreaves behavioral test measures the response to thermal stimulation, which is mediated by small, unmyelinated C fibers.[3-4] A focused infrared beam, increasing in intensity at ~ 0.3°C/s, was emitted under the plantar surface of alternating hind paws; individual readings were taken approximately every five minutes to avoid hyperalgesia. The amount of time required to induce paw withdrawal (seconds) was recorded and averaged (four measurements/animal). The Hargreaves apparatus was calibrated prior to acclimation using a heat flux radiometer (Ugo Basile, Comerio, Italy).

VI. ASSESSMENT OF MECHANICAL SENSITIVITY

The Dynamic Plantar Anasethesiometer (Ugo Basile, Comerio, Italy) was used to monitor response to mechanical stimuli. The Von Frey behavioral test measures mechanical response to a stiff monofilament applied to the plantar surface. Detection of mechanical stimulation is mediated by thinly myelinated Aδ nerve fibers.[5] The Von Frey monofilament consists of a 0.5 mm diameter steel fiber attached to a force actuator. Mice were placed within a covered plastic cubicle that rested upon a wire mesh platform and allowed to acclimate for 30-40 minutes. Upon activation, the anethesiometer applied the tip of the monofilament to the plantar surface of alternating hind paws at an upward force of 8 g at a ramping speed of 2 s. A series of five recordings were taken every five minutes, measuring the force (grams) necessary to elicit paw withdrawal and the latency associated with this response. The five recordings from each animal were averaged. The anesthesiometer was calibrated using a 50 g steel weight prior to specimen acclimation.

VII. NERVE CONDUCTION VELOCITY

All nerve conduction velocity measurements were conducted in accordance with published protocols.[6] Mice were anesthetized via IP injection of either 75 mg/kg Nembutal or 100 mg/kg ketamine with 10 mg/kg xylazine. Animals were only operated upon after confirmation of surgical anesthesia using the eye blink reflex method. Motor and sensory nerve conduction velocities were measured using a TECA™ Synergy N2 (Carefusion, San Diego, CA) system with 12 mm subdermal disposable platinum/iridium bipolar needle electrodes (Cardinal Health Neurocare, Madison, WI). Body temperature was monitored using a rectal probe and Physitemp TCAT-2DF Controller (Physitemp Instruments, Clifton, NJ) and maintained at 37°C using a heat lamp.

Motor Nerve Conduction Velocity (MNCV)

A stimulatory electrode was placed either within the sciatic notch (proximal) or above the calcaneous and ventral to the achilles tendon (distal). A recording electrode was inserted into the first interosseous muscle of the hind paw. Three additional electrodes were placed within adjacent tissues to improve the signal:noise ratio. Electrical stimulation consisted of a 9.9 mA 0.05 ms duration square wave. The resulting waveforms were filtered with low and high settings of 3 and 10 kHz, respectively. Latencies were defined as the time between stimulus artifact and the onset of negative M-wave deflection. MNCV (m/s) was calculated by dividing the difference between proximal and distal latencies by the distance between stimulating and recording electrodes. Three MNCV values were determined and averaged.

Sensory Nerve Conduction Velocity (SNCV)

A stimulatory electrode was inserted into the tip of the second hind toe and, upon stimulation, delivered a 2.4-3.0 mA 0.05 ms square wave pulse that traveled to the receiving electrode behind the medial malleolus. The resulting wavelengths were filtered with low and high settings of 3 and 10 kHz, respectively. A series of ten sensory nerve action potential measurements were taken and averaged to generate a single waveform. Latency was determined as the change in time between stimulus artifact to the onset of peak negative deflection. SNCV was determined by dividing latency by the distance between stimulating and receiving electrodes.

VIII. EUTHANIZATION AND TISSUE HARVESTING

All animals were euthanized in accordance with NIH guidelines and IACUC pre-approved protocols. Upon completing the NCV measurements, animals were euthanized by cardiac excision followed by prompt decapitation. Animals not subject to NCV were euthanized via CO_2 asphyxiation. Select organs and tissues were collected immediately.

Sciatic, tibial, and sural nerves were dissected from both hind limbs, cut into smaller segments, and added to 0.2 ml mRIPA (modified radioimmunoprecipitation assay) buffer (50 mM Tris-HCl, pH 7.5, 1 mM EDTA, 1% Nonidet P-40, 0.5% deoxycholate, 0.1% SDS, 150 mM Na_2VO_3, 0.5 mM Na_2MoO_4, 40 mM NaF, and 10 mM β-glycerophosphate) with 1X complete protease inhibitor cocktail (Roche Diagnostics) on ice. The tissue was homogenized with a Polytron fitted with a micro tissue tearor and centrifuged at 10,000 x g at 4°C for 10 minutes. The supernatant was

collected, flash frozen on dry ice, and stored at – 20°C. Sensory dorsal root ganglia were dissected and collected near the L1-L6 lumbar vertebrae using a dissection microscope. DRG protein samples were collected and stored in the same manner described above for the nerves.

Blood samples were vortexed with an anticoagulant (50 µl 0.3 M ethylenediaminetetraacetic acid (EDTA)) with 1X complete protease inhibitor cocktail and centrifuged at 1,500 x g at 4°C for 10 minutes. Blood serum (supernatant) was collected and flash frozen on dry ice. Kidney, liver, brain, and pancreas samples were also collected and frozen with dry ice and stored at – 80°C.

The plantar integument (foot pads) of both hind paws were dissected and fixed using Zamboni's fixative (3% paraformaldehyde, 15% picric acid) (Newcomer Supply, Middleton, WI) overnight at 4°C. Foot pads were rinsed 2-3 times with cold (4°C) PBS buffer with 3 mM NaN_3, pH 7.4. All tissues were then incubated in 30% sucrose (cryoprotectant) overnight in 4°C and subsequently embedded in Tissue-Tek optimal cutting temperature compound (OCT) (Sakura USA, Torrence, CA) on dry ice and stored at – 80°C. Frozen samples were cut into 30 µm sections, placed on Fisherbrand Superfrost Plus microscope slides, and stored at – 80°C until immunohistochemistry was performed to analyze intraepidermal nerve fiber density.

IX. INTRAEPIDERMAL NERVE FIBER DENSITY (IENFD)

IENFD analysis was conducted using the Vectastain Elite ABC-Peroxidase kit for rabbit IgG (Vector Laboratories, Burglingame, CA) and anti-PGP 9.5 primary antibody (AbD Serotec, Raleigh, NC). Slides were blocked using goat serum for 30

minutes and incubated with anti-PGP 9.5 antibody (1:1,000 dilution) at room temperature for three hours. The slides were then rinsed with PBS, incubated with secondary antibody for one hour at room temperature, and further rinsed with cold PBS. All slides were then incubated in ABC (avidin-biotin complex) solution for one hour at room temperature, rinsed with PBS, and incubated with NovaRED peroxidase substrate solution (Vector Laboratories, Burlingame, CA) for 2-3 minutes. The sections were counterstained with hematoxylin (Vector Laboratories, Burlingame, CA), coverslipped, and imaged using Zeiss Axioplan-2 light microscope (Carl Zeiss Microimaging, Thornwood, NY) and a color ccd digital camera (Diagnostic Instruments Inc., Sterling Heights, MI). Three images were captured from two different sections of two representative slides per animal (*i.e.* 12 images/animal). The number of nerve fibers crossing the dermal/epidermal junction (immunopositive) were normalized to the quantified segment length.

X. INSULIN ELISA

Insulin blood serum concentrations were quantified using the Mercodia Mouse Insulin ELISA (Enzyme-linked immunosorbent assay) kit (Mercodia AB, Uppsala, Sweden). Briefly, serum protein concentration was quantified using the Bio-Rad Protein Assay (Bio-Rad Laboratories, Inc., Hercules, CA) and equivalent amounts of protein were diluted to 25 µl (mRIPA with 1X protease inhibitors) and added in triplicate to the 96-well ELISA plate containing bound anti-insulin antibodies. ELISA calibrators and control insulin stock concentrations were employed to establish a calibration curve and serve as positive controls. 50 µl of peroxidase-conjugated anti-

insulin antibody solution was added and incubated on a shaker (800 rpm) for two hours at room temperature. Each well was subsequently washed six times with 0.35 ml wash buffer, inverted on paper, and allowed to dry. 0.2 ml of 3,3',5,5'-tetramethylbenzidine (TMZ) solution was added to each well and incubated for 15 minutes in the dark. The reaction was stopped with the addition of 50 µl 0.5 M H_2SO_4, vortexed for 5-10 seconds, and the absorbance at 450 nm (A_{450}) was read using a UV-Vis spectrometer. The calibration curve was used to determine serum insulin concentrations within the collected samples.

XI. IMMUNOBLOT ANALYSIS

Immunoblot (western blot) analyses were performed on neural tissue homogenates.[7] Protein samples were thawed on ice and quantified via the Bradford assay. 20 µg of protein was separated using SDS-PAGE (sodium dodecyl sulfate-polyacrylamide gel electrophoresis), transferred to nicrocellulose membrane, and stored in PBS-T (PBS buffer with Tween) at 4°C. Membranes were blocked with three 20-minute washes of 5% milk in PBS-T via gentle rocking. Membranes were then incubated with primary antibodies overnight at 4°C, with the exception of β–actin (two hours at room temperature). Membranes were then washed in 5% blocking buffer three times for ten minutes each. Upon completion, membranes were incubated with secondary antibodies for 1 hour (β–actin) at room temperature or 3 hours (all others) at 4°C. The membranes were then washed three times for five minutes with PBS-T and incubated with an HRP-conjugated chemiluminescence detection kit (ECL Plus Western Blotting Detection Reagents, Amersham Biosciences, Buckinghamshire,

UK). Autoradiography film was exposed to the chemiluminescent signal, developed, and the bands were quantified via densitometry using ImageJ software. Protein levels were normalized to β-actin and control treatments.

Table 2.1. Antibodies used in the analyses.

Antibody	Manufacturer	Catalog
β-actin	Santa Cruz Biotechnology	sc-47778
Hsp72	Stressgen Assay Designs	SPA-810
Hsp90	Stressgen Assay Designs	SPA-830
nNOS (NOS-1)	Santa Cruz Biotechnology	sc-5302
PGP 9.5	AbD Serotec	7863-0504
Goat anti-Rabbit HRP	Santa Cruz Biotechnology	sc-2004
Goat anti-Mouse HRP	Santa Cruz Biotechnology	sc-2005

XII. STATISTICAL ANALYSIS

Data are presented as mean ± SEM. After verifying equality of variances, differences between treatments were determined using factorial ANOVA. Differences between group means were ascertained using Tukey HSD posthoc test. Statistical analyses were performed using Systat 12 (Systat Software, Chicago, IL) and portrayed using Graphpad Prism (Graphpad Software, Inc., La Jolla, CA).

XIII. References

1. American Diabetes Association, *Diabetes Care* **2010,** *33 Suppl 1*, S4-10.
2. Burlison, J. A.; Neckers, L.; Smith, A. B.; Maxwell, A.; Blagg, B. S., *J Am Chem Soc* **2006,** *128* (48), 15529-36.
3. Hargreaves, K.; Dubner, R.; Brown, F.; Flores, C.; Joris, J., *Pain* **1988,** *32* (1), 77-88.
4. Yeomans, D. C.; Proudfit, H. K., *Pain* **1996,** *68* (1), 141-50.
5. Julius, D.; Basbaum, A. I., *Nature* **2001,** *413* (6852), 203-10.
6. McGuire, J. F.; Rouen, S.; Siegfreid, E.; Wright, D. E.; Dobrowsky, R. T., *Diabetes* **2009,** *58* (11), 2677-86.
7. Bradford, M. M., *Anal Biochem* **1976,** *72*, 248-54.

CHAPTER 3: EXPERIMENTAL DESIGN

In order to test *in vivo* efficacy of KU-32 against several clinical measures of diabetic peripheral neuropathy, several studies were conducted using the template depicted in Figure 3.1. This template outlines the standard procedures employed during chronic 12-week intervention studies. However, several studies were conducted to analyze KU-32 affects in more acute disease states (*i.e.* 8-week intervention studies), the effects of dose variation, and preliminary toxicity studies spanning six weeks in non-diabetic mice. Regardless, Figure 3.1 depicts the general format of all studies.

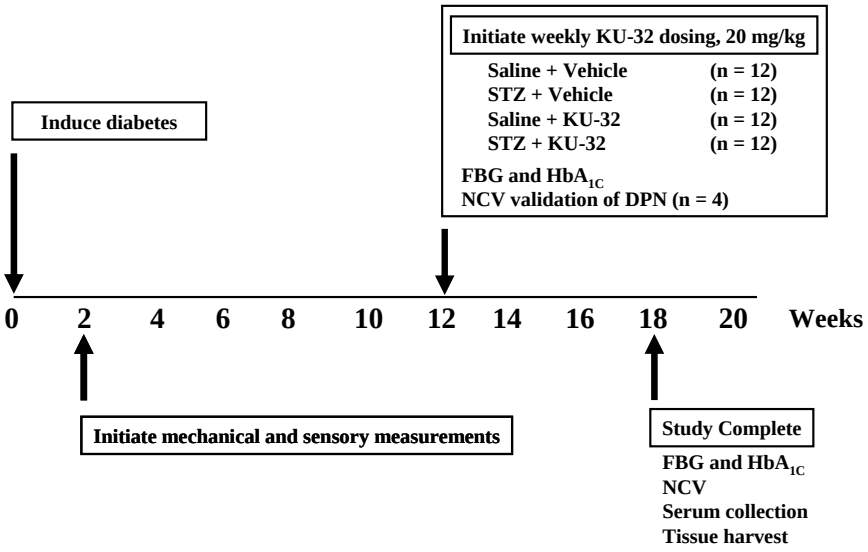

Figure 3.1. Experimental design of 12-week intervention study.

In 12-week intervention studies, mice were rendered diabetic at 7-8 weeks of age. The standard population size (n) per test group was generally established at twelve or greater. When possible, mice were equally divided by gender and body weight across all treatment groups. Two weeks after the induction of diabetes,

Hargreaves and Von Frey behavioral testing were initiated after the progressive development of sensorimotor deficits. At twelve weeks, select control and diabetic mice were administered 20 mg/kg KU-32 or vehicle on a weekly basis for six weeks. Fasting plasma glucose levels and HbA_{1C} levels were monitored to verify altered metabolic states prior to and at the conclusion of KU-32 administration. Motor and sensory nerve conduction velocities were measured for benchmark specimens (four per treatment group) prior to KU-32 administration, and organs/tissues were extracted, harvested, and stored for comparison with samples collected at the end of the study. Upon study completion at 18 weeks, MNCV and SNCV levels were measured for all mice and organs/tissues were extracted, harvested and stored. Blood and tissue samples were subsequently analyzed for protein content and innervation via immunohistochemistry (IENFD).

CHAPTER 4: RESULTS

I. PRELIMINARY ASSESSMENTS

Initial screens were conducted in wild-type (WT) eight-week old C57 Bl/6 mice through weekly IP injections of 2 mg/kg KU-32, 20 mg/kg KU-32, or vehicle for six weeks. KU-32 treatment alone did not significantly alter mechanical or thermal sensitivity, MNCV, or SNCV (Figure 4.1) when compared to non-treated control mice. Thus, KU-32 had no affect on altering common measures of neuropathy. Affects of KU-32 on murine body weight were also analyzed during this study to identify any abnormal, drug-induced weight fluctuations that may pose additional metabolic complications (Figure 4.2). KU-32 did not alter body weight.

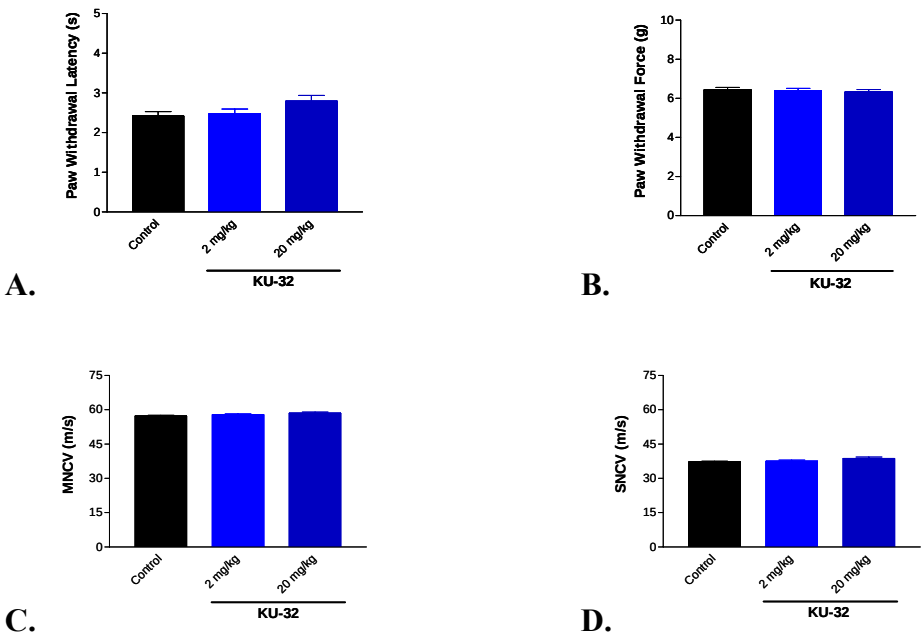

Figure 4.1. Preliminary *in vivo* assessments of KU-32 in wild-type C57 Bl/6 mice. C57 Bl/6 mice were administered weekly IP injections of 2 mg/kg KU-32, 20 mg/kg KU-32, or 0.1 M Captisol equivalent vehicle (Control) over six weeks. KU-32 displayed no alterations in (A) thermal and (B) mechanical sensitivity, nor changes in (C) MNCV or (D) SNCV. $p > 0.05$ versus control.

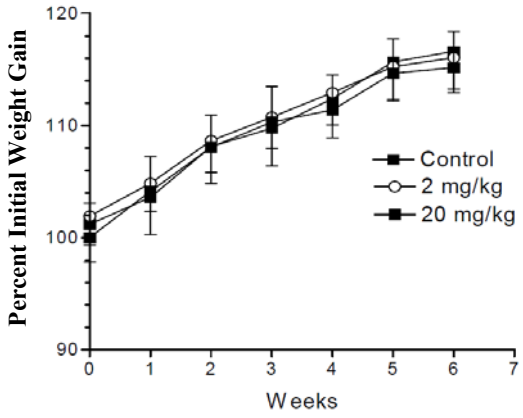

Figure 4.2. Preliminary assessment of KU-32 on body weight. KU-32 had no affect on mouse body weight.

II. KU-32 IMPROVES EXPERIMENTAL DIABETIC PERIPHERAL NEUROPATHY

In order to assess the potential efficacy of KU-32 *in vivo*, we induced Type I diabetes in wild-type C57 Bl/6 mice and allowed sensorimotor deficits to progress over the course of 12 weeks. Diabetic animals clearly developed negative neurodegenerative symptoms by 12 weeks, where diabetic mechanical responses averaged 7.2 ± 0.5 g (5.7 ± 0.3 g control) and thermal responses were at 7.9 ± 0.6 s (5.4 ± 0.2 s control) (Figure 4.3). However, upon completion of the 6-week KU-32 treatment regimen (20 mg/kg KU-32 administered weekly), diabetic animals demonstrated a near complete recovery in both mechanical and thermal sensitivity. KU-32 improved mechanical sensitivity in diabetic mice to 5.8 ± 0.8 g (7.7 g STZ; 5.6 ± 0.4 g control) and thermal sensitivity to 6.2 ± 0.6 s (7.7 s STZ; 5.8 ± 0.1 s control). This suggests that KU-32 improved both thinly myelinated and unmyelinated nerve fibers at more chronic phases of DPN. KU-32 did not alter mechanical or thermal sensitivity in control untreated mice.

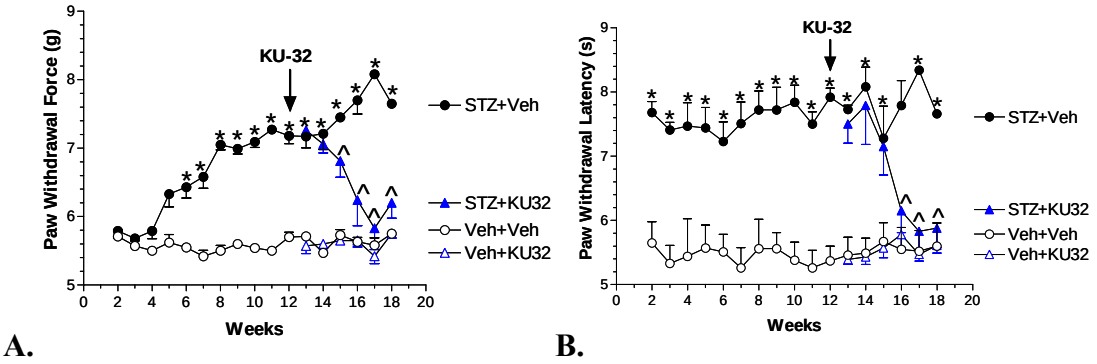

A. **B.**

Figure 4.3. Mechanical and thermal hypoalgesia in 12-week intervention studies. Diabetes was induced with STZ in wild-type C57 Bl/6 mice and sensorimotor deficits were allowed to develop for 12 weeks. Select diabetic and control mice were then treated with weekly IP injections of 20 mg/kg KU-32 or vehicle for six weeks. KU-32 restored normal behavioral responses in diabetic mice in both (A) mechanical and (B) thermal sensitivity. *, $p < 0.05$ compared to the time matched control; ^, $p < 0.05$ compared to time matched STZ + Veh.

Motor and sensory nerve conduction velocities were also measured to assess KU-32's potential impact upon nerve conduction. At 12 weeks, nerve conduction velocities significantly declined in diabetic animals to 82.0 ± 10.4% MNCV and 91.0 ± 4.4% SNCV relative to control animals (Figure 4.4). This decrease became more prominent as the disease progressed to study completion at 18 weeks with 74.4 ± 8.8% MNCV and 84.2 ± 5.6% SNCV. While KU-32 did not alter NCV's in control mice, KU-32 significantly recovered diabetic NCV to 93.6 ± 4.8% MNCV and 98.7 ± 6.7% SNCV. Therefore, KU-32 reversed pre-existing conduction deficits observed in diabetic motor and sensory nerve fibers and prevented the further decline in NCV that occurred between 12 to 18 weeks of diabetes.

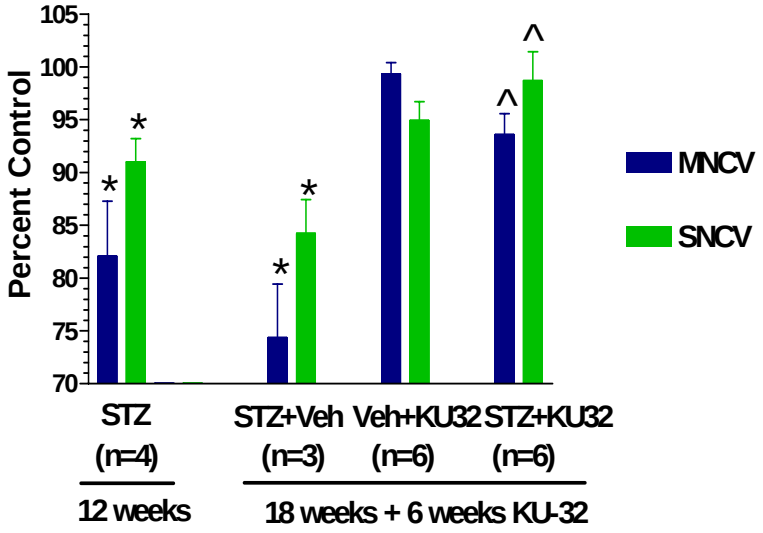

Figure 4.4. MNCV and SNCV in 12-week intervention studies. Motor and sensory nerve conduction velocities were conducted in anesthetized mice at 12 and 18 weeks to assess neurodegeneration prior to and after KU-32 administration. MNCV and SNCV were normalized to vehicle-treated control mice at 12 and 18 weeks (expressed as percent control). KU-32 restored diabetic MNCV and SNCV to within 95-100% of control NCV. *, $p < 0.01$ versus time-matched untreated control; ^, $p < 0.001$ versus 18 week STZ + Veh; Control MNCV: 60.4 $\pm$ 2.0 m/sec; Control SNCV: 39.3 $\pm$ 1.9 m/sec.

Since KU-32 improved several of the standard clinical indices of negative symptoms associated with small and large fiber dysfunction, the next question became "How does KU-32 exert these neuroprotective effects?" We proposed that KU-32 may alter dysfunctional metabolic control mechanisms within diabetic animals. To test this hypothesis, we measured HbA_{1C} and FBG levels prior NCV and conducted an insulin ELISA to measure insulin content within serum samples collected perimortem. As expected, HbA_{1C} and FBG levels were elevated in diabetic animals, averaging 11.8 ± 0.3% (4.7 ± 0.1% control) and 389 ± 83 mg/dl (135.7 ± 3.9 mg/dl control), respectively (Figure 4.5.A.). Insulin concentrations were 2.5-fold greater in control animals (0.25 ± 0.13 nM) versus diabetic animals (0.10 ± 0.01 nM) (Figure 4.5.B.)

(*n.b.* complete annihilation of insulin production is lethal). KU-32 had no impact upon any of these clinical indicators, suggesting that the compound doesn't rejuvenate metabolic control.

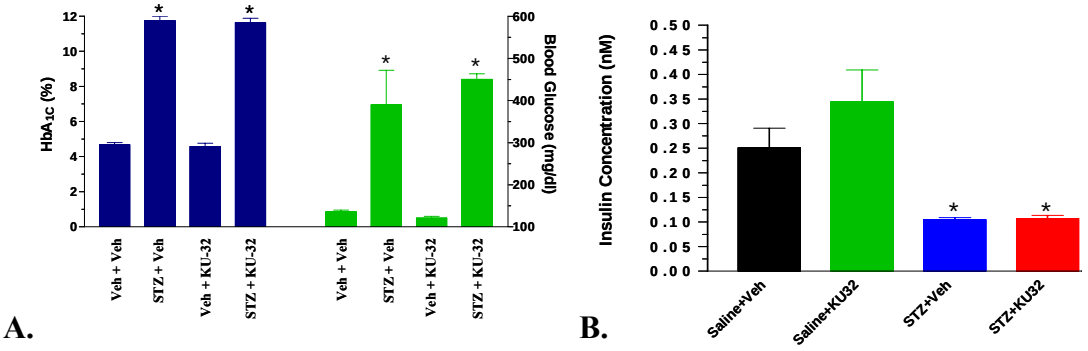

Figure 4.5. HbA_{1C}, FBG, and insulin levels in 12-week intervention studies. (A) Percent glycated hemoglobin levels (HbA_{1C}) and fasting plasma glucose levels were measured prior to anesthetic administration for NCV studies. (B) Insulin concentrations were determined using an insulin ELISA for samples collected perimortem. KU-32 had no impact upon metabolic control. *, $p < 0.05$ versus Veh + Veh.

To confirm this notion, we tested whether prophylactic treatment of KU-32 could modify the rate of blood glucose clearance within wild-type C57 Bl/6 mice (Figure 4.6). FBG levels were measured three days after the IP administration of 20 mg/kg KU-32 or vehicle (t = 0 min). A glucose bolus (2 g/kg in 200 µl sterile 1XPBS) was injected (IP) and plasma glucose levels were measured through the duration of two hours. Although there was a slight significant deviation at ten minutes with KU-32 treatment, the glucose concentrations of both treatments converged to normal basal levels simultaneously at two hours. This reconfirmed that KU-32 doesn't impact systemic metabolic control.

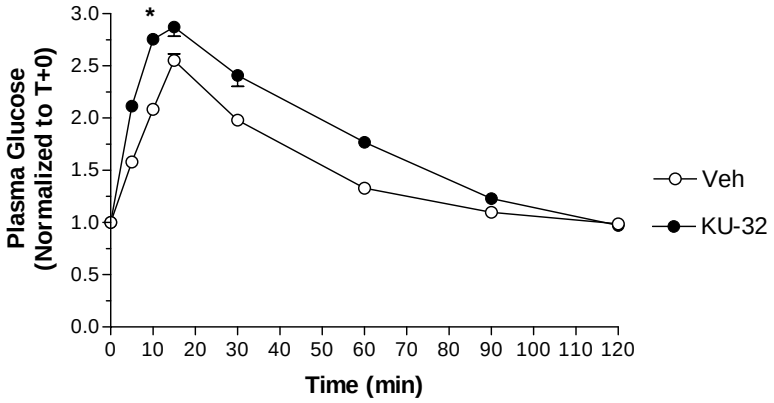

Figure 4.6. Plasma glucose clearance of glucose in KU-32 pretreated mice. C57 Bl/6 mice were administered an intraperitoneal injection of 20 mg/kg KU-32 or vehicle three days prior to the metabolic study. Baseline FBG levels were measured prior to glucose administration (t = 0 min). Control and KU-32-treated mice were administered a glucose bolus (2 g/kg glucose in 0.2 ml sterile 1X PBS) via IP injection. Plasma glucose levels were monitored through the course of 2 hours. All measurements were normalized to basal measurements taken prior to glucose injection; *, $p < 0.05$ versus time-matched untreated control; n = 6 per group.

These data suggested that hyperglycemia may adversely impact the folding/refolding capabilities of newly synthesized or mildly damaged proteins within peripheral neurons. Therefore, we investigated whether the removal of heat shock proteins would enhance DPN progression or negate KU-32 efficacy.

III. KU-32 EFFICACY IN HSP70.1/HSP70.3 DOUBLE KNOCKOUT MICE

Since Hsp90 knockouts are non-viable, we elected to test the affects of KU-32 in Hsp70 double knockout mice. As reviewed in section I, Hsp70 induction can afford several neuroprotective attributes, including Hsp90-dependent and -independent client protein folding/refolding, trafficking, and ubiquitination. Therefore, we repeated the 12-week intervention study in Hsp70 double knockout mice, in which both inducible isoforms, Hsp70.1 and Hsp70.3, were removed.

Similar to wild-type C57 Bl/6 mice, diabetic Hsp70 double knockout (Hsp70 KO) mice developed noticeable sensorimotor deficits (Figure 4.7). At 12 weeks, diabetic mechanical responses averaged 7.3 ± 0.5 g (5.6 ± 0.4 g control) and thermal responses were at 8.2 ± 1.2 s (5.3 ± 0.4 s control). However, Hsp70 KO mice did not respond to the KU-32 treatment. Although there were some slight fluctuations in mechanical and thermal sensitivity at weeks 13-15, these were primarily attributed to attrition within the diabetic population. Mechanical sensitivity also decreased at weeks 15-17 in non-diabetic KU-32-treated mice. However, these deviations subsided by the conclusion of the study.

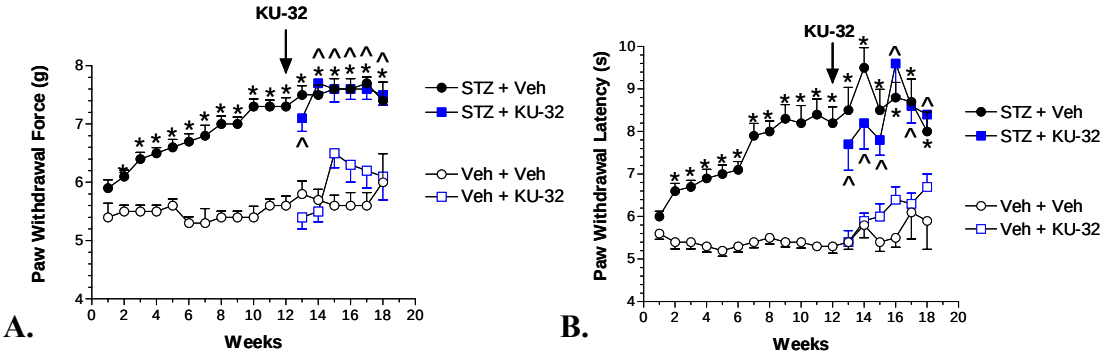

Figure 4.7. Mechanical and thermal sensation in 12-week intervention Hsp70 KO mice. Diabetes was induced with STZ in Hsp70.1/Hsp70.3 double knockout mice and sensorimotor deficits were allowed to develop for 12 weeks. Select diabetic and control mice were then treated with weekly IP injections of 20 mg/kg KU-32 or vehicle for six weeks. KU-32 had no affect in diabetic mice for both (A) mechanical and (B) thermal sensitivity. *, indicates $p < 0.01$ compared to Veh + Veh; ^, indicates $p < 0.01$ compared to Veh + KU-32; n = 4-6 per group.

Diabetic Hsp70 KO mice also exhibited a 15-20% decline in both MNCV and SNCV relative to vehicle-treated non-diabetic mice (Figure 4.8). Weekly KU-32 administration failed to improve MNCV and SNCV in Hsp70 KO mice.

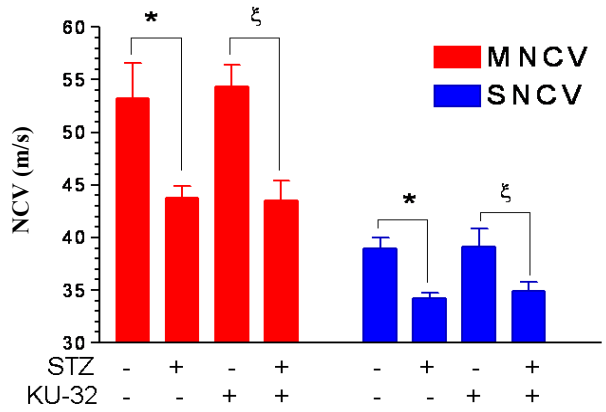

Figure 4.8. MNCV and SNCV in 12-week intervention Hsp70 KO studies. Motor and sensory nerve conduction velocities were conducted in anesthetized mice at 12 and 18 weeks to assess neurodegeneration prior to and after KU-32 administration in Hsp70.1/Hsp70.3 double knockout mice. KU-32 did not improve deficits in either motor or sensory nerve conduction velocities. *, indicates $p<0.01$ compared to minus STZ and KU-32; ξ, $p < 0.01$ compared to minus STZ and KU-32; n = 4-6 per group.

The deletion of inducible Hsp70 had no significant impact upon systemic metabolic control (Figure 4.9) in either diabetic or control mice. Comparable to WT C57 Bl/6 mice, KU-32 administration did not alter vascular HbA_{1C} or plasma glucose levels in Hsp70 KO mice.

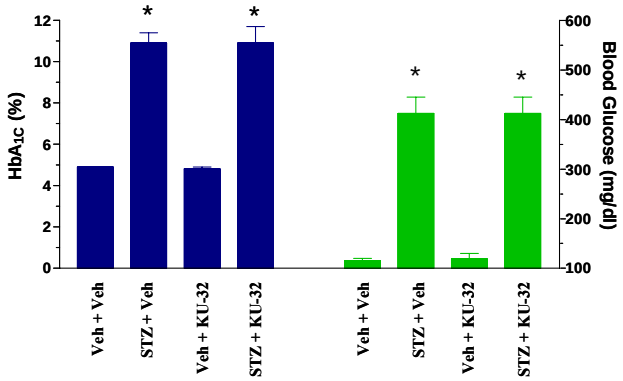

Figure 4.9. HbA_{1C} and FBG in 12-week intervention Hsp70 KO mice. HbA_{1C} and FBG levels were measured prior to anesthetic administration for NCV studies. KU-32 had no impact upon metabolic control. *, $p < 0.05$ versus Veh + Veh.

Collectively, these data imply that inducible Hsp70 is essential for KU-32-mediated neuroprotective effects. It also suggests that the elimination of functional, inducible Hsp70 isn't enough to drive or enhance pathophysiological progression.

IV. KU-32 DOSE-VARIATION STUDIES

Since KU-32 was effective at improving several of the negative symptoms associated with DPN, we decided to test the potency of KU-32 through dose-variation studies in more acute studies. We conducted an 8-week intervention study in which we treated diabetic and non-diabetic WT C57 Bl/6 mice with either 2.0 mg/kg KU-32, 0.2 mg/kg KU-32, or vehicle. A separate study was also conducted that explored the affects of 20 mg/kg KU-32 in an identical 8-week intervention study. Differences between investigators and data collection techniques prevented the comparison of behavioral data between the two studies. However, NCV studies and metabolic parameters can be compared and will be discussed below.

In the low-dose (0.2 mg/kg and 2.0 mg/kg KU-32) 8-week intervention study, we observed normal sensorimotor deficit progression in both mechanical and thermal sensitivity observed in the 12-week intervention study in the diabetic animals (Figure 4.10). Prior to drug administration at week 8, mechanical responses in diabetic animals were at 7.5 ± 0.2 g (5.8 ± 0.3 g control) and thermal responses were at 9.4 ± 1.1 s (5.4 ± 0.4 s control). Diabetic mice administered KU-32 exhibited a dose-dependent recovery in mechanical sensitivity from 7.7 ± 0.2 g (STZ + Veh) to 7.2 ± 0.4 g (STZ + 0.2 mg/kg KU-32) and 6.7 ± 0.6 g (STZ + 2.0 mg/kg KU-32) in comparison to non-diabetic mice (5.7 ± 0.2 g Veh + Veh). In contrast, treatment with

0.2 mg/kg KU-32 only slightly improved thermal responsiveness at weeks 12-13 to 9.3 ± 1.7 s (11.5 ± 0.8 s STZ + Veh; 5.6 ± 0.3s Veh + Veh); 2 mg/kg KU-32 improvements were just outside statistical significance. This suggests that the neuroprotective effects induced by KU-32 may be dose-dependent and vary according to cell or fiber type.

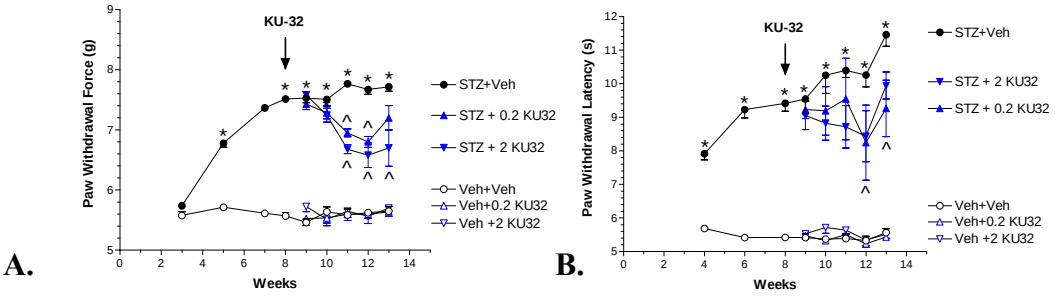

Figure 4.10. Mechanical and thermal sensation in 8-week intervention dose-variation studies. Diabetes was induced with STZ and sensorimotor deficits were allowed to progress over 12 weeks. Select diabetic and control mice were then treated with weekly IP doses of 0.2 mg/kg KU-32, 2.0 mg/kg KU-32, or vehicle for six weeks. KU-32 displayed a dose-dependent recovery in (A) mechanical sensitivity and 0.2 mg/kg KU-32 slightly altered (B) thermal sensitivity. *, $p < 0.05$ compared to the time matched control; ^, $p < 0.05$ compared to time matched STZ + Veh.

Assorted KU-32 treatments in the 8-week intervention study displayed a dose-dependent response in MNCV and substantially improved SNCV (Figure 4.11). Although 0.2 mg/kg and 2 mg/kg KU-32 did not affect MNCV, 20 mg/kg KU-32 significantly improved MNCV to 54.0 ± 1.8 m/s (44.4 ± 0.2 m/s STZ + Veh; 57.2 ± 0.5 m/s Veh + Veh). 0.2 mg/kg and 20 mg/kg KU-32 treatment improved SNCV to 39.9 ± 1.5 m/s and 39.0 ± 1.3 m/s, respectively (35.1 ± 0.5 m/s STZ + Veh; 39.5 ± 0.3 m/s Veh + Veh) (Figure 4.11A.). The 2 mg/kg KU-32 treatment data depicts only two measurements that were able to taken due to STZ-induced mortality. Hence,

increasing n would most likely improve SNCV within this treatment group. As expected, KU-32 had no significant impact upon HbA_{1C} and FBG levels (Figure 4.12).

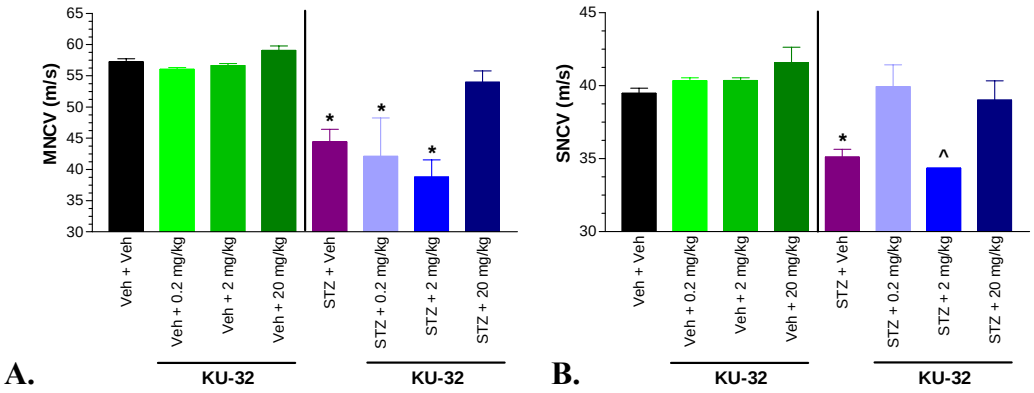

Figure 4.11. MNCV and SNCV in 8-week intervention dose-variation studies. Motor and sensory nerve conduction velocities were conducted in anesthetized mice at 14 weeks to assess neurodegeneration after KU-32 administration in WT C57 Bl/6 mice. KU-32 improved (A) MNCV deficits at 20 mg/kg KU-32 and (B) SNCV deficits at 0.2 and 20 mg/kg (*n.b.* n = 2 for 2 mg/kg KU-32). *, $p < 0.001$ compared to Veh + Veh; ^, too few values.

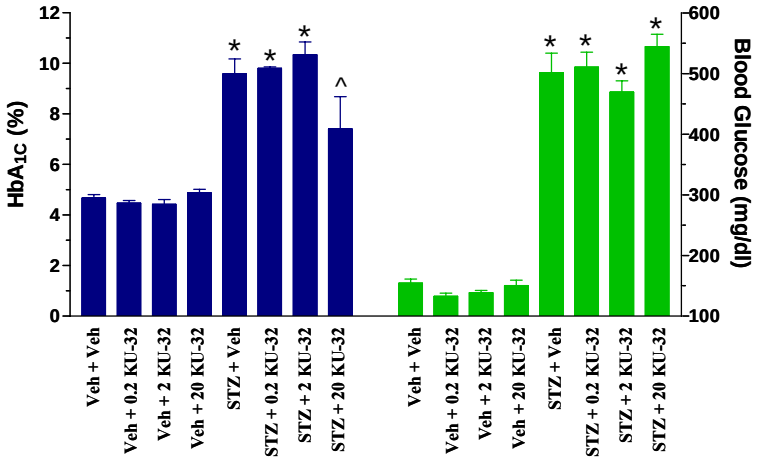

Figure 4.12. HbA_{1C} and FBG in 8-week intervention dose-variation studies. HbA_{1C} and FBG levels were measured prior to anesthetic administration for NCV studies. KU-32 had no impact upon metabolic control. *, $p < 0.001$ versus Veh + Veh control; *, $p < 0.05$ versus Veh + Veh control.

V. INTRAEPIDERMAL NERVE FIBER DENSITY (IENFD)

Foot pad samples were collected from the hind paws of both WT and Hsp70 KO 12-week intervention studies in order to analyze whether KU-32 could alter sensory nerve fiber density. Immunohistochemistry was used to determine the number of nerve fibers that crossed the dermal/epidermal junction (expressed as a function of segment length) (Figure 4.13). Surprisingly, at 18 weeks of STZ-induced diabetes, neither WT nor Hsp70 KO mice exhibited any significant changes in IENFD. Nevertheless, this data does show that KU-32 has no positive or negative impacts upon nerve fiber density in both healthy and diabetic mice within the first six weeks of treatment.

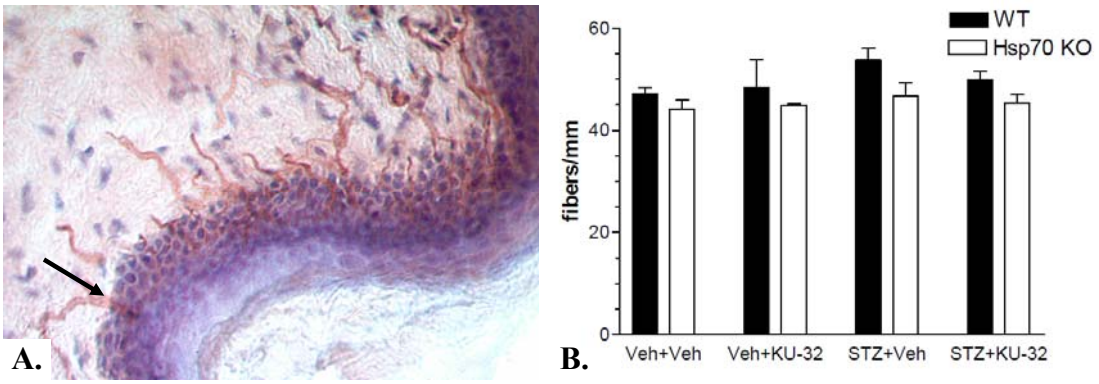

Figure 4.13. Epidermal innervation in diabetic and non-diabetic mice before and after treatment in 12-week intervention studies. Foot pad samples were collected from the hind paws of representative mice of each treatment group WT and Hsp70 KO 12-week intervention studies. Foot pad samples were subsequently cut, stained, imaged, and analyzed for IENFD. (A.) Representative image from a non-KU-32-treated mouse. Epidermal cells are stained purple and nerve fibers are stained red (arrow). (B.) The number nerve fibers penetrating the epidermis were quantified and normalized to the length of the epidermal surface in the field of view. Neither STZ nor KU-32 treatment had a significant impact on IENFD in both WT and Hsp70 KO mice. n = 4 mice per treatment at 12 images each.

VI. IMMUNOBLOT ANALYSES

Western blot analysis was conducted to measure the affects of KU-32 on protein expression. Hsp90 and Hsp70 expression levels varied significantly between and within treatment groups. Figure 4.14 shows several representative immunoblots conducted on neuronal tissue samples (sciatic, sural, and tibial nerves) that were collected at the end of the WT 12-week intervention study. Although Hsp70 was induced in some animals (animal set #1, Figure 4.14.A.), other animals within the same treatment group (animal set #2, Figure 4.14.B.) displayed no upregulation. Hsp90 expression levels also fluctuated near/around basal levels (Figure 4.14.C). Therefore, it's possible that the effects elicited by KU-32 may be more transient in nature and are merely missed since we took the tissues at the completion of the studies. Although KU-32 was found to significantly downregulate neuronal nitric oxide synthase (nNOS) (Figure 4.14.D) in diabetic mice, the majority of altered protein expression levels in nerve and DRG homogenates has remained modest or relatively inconsistent. Current studies are being conducted to further analyze transient protein effects.

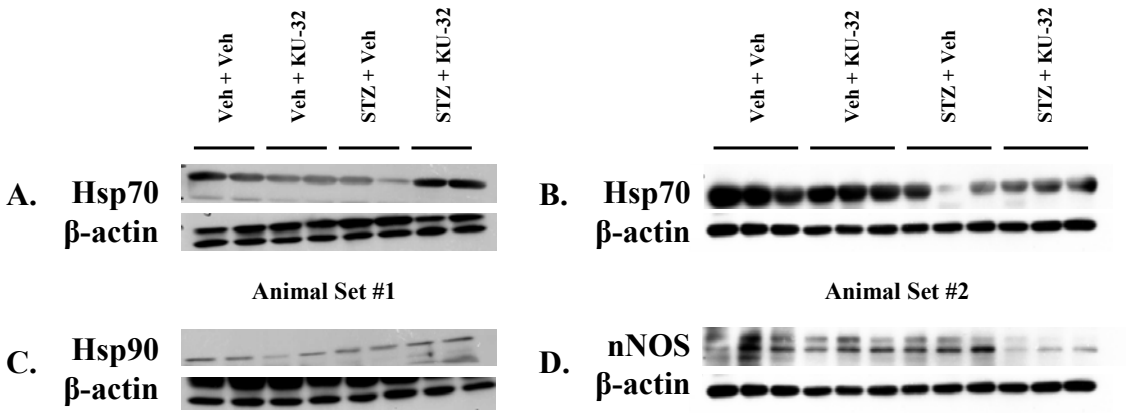

Figure 4.14. Immunoblot analysis of nerve tissue homogenates in the WT 12-week intervention study. Neuronal tissue homogenates from the WT 12-week intervention study were analyzed via immunoblotting for (A-B) inducible Hsp70, (C) Hsp90, and (D) nNOS. Two sets of animals from the same treatment group are displayed.

CHAPTER 5: DISCUSSION AND CONCLUSION

We have shown that KU-32 improves several standard clinical indices of negative symptoms associated with small and large fiber dysfunction in the absence of improving overall metabolic control. The affects of KU-32 appear to be dose-dependent and require the presence of inducible Hsp70 for efficacy. These data also indicate that inducible Hsp70 is not required for the pathophysiological progression of diabetic peripheral neuropathy. However, this doesn't eliminate the potential involvement of other Hsp70 family members as Hsc70 displays a certain degree of interchangeability with inducible Hsp70. Regardless, Hsp70 KO mice develop sensorimotor deficits at a similar rate and severity in comparison to WT C57 Bl/6 mice. It still remains to be determined whether KU-32 induces HSF-1-mediated heat shock response. Recent *in vitro* data (not presented) suggests that induction of the HSR may be less pronounced in different cell types and its potency may vary accordingly as well. However, the resounding question still reverberates: "How does KU-32 provide neuroprotection in DPN?" To answer this question, one must first examine the tentative binding site of KU-32.

I. HYPOTHETICAL MECHANISMS OF ACTION

KU-32 is a descendent of A4-inspired novobiocin analogs. A4 is the 8-desmethyl version of KU-32 that was originally designed as an Hsp90 inhibitor (Figure 5.1).[1] A4 binds within the C-terminal nucleotide-binding domain and induces Hsp70 expression at concentrations 1,000-10,000-fold lower than that needed to induce client protein degradation and associated cytotoxicity.[1] It is currently

hypothesized that novobiocin binds to the C-terminal nucleotide-binding domain, disrupts co-chaperone associations (Hsc70 and p23), and extends into the Hsp90 dimerization domain, infringing on dimerization.[2-3] However, this has not been proven. SAR (structure-activity relationship) studies have demonstrated that replacement of the benzamide sidechain with an acetamide significantly reduces cytotoxicity.[2, 4] It's hypothesized that the benzamide sidechain is responsible for disrupting dimerization. Since A4 and KU-32 lack this moiety, it's speculated that these compounds bind in a similar fashion to novobiocin but induce allosteric modulation versus dimer disruption. This allosteric modulation may drive HSF-1 dissociation and induce the heat shock response.

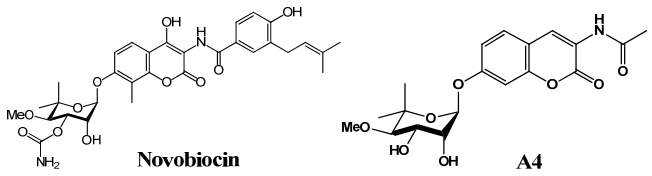

Figure 5.1. Structures of novobiocin and A4.

Examination of the tentative KU-32-binding site via molecular modeling reveals several readily accessible hydroxyl-containing amino acids that may be subject to post-translational modifications (PTMs): Y690, T540, S543, T594, S595, Y492, and Y493. These potential interactions were identified using a molecular model created by The Center for Bioinformatics at The University of Kansas (unpublished data). Briefly, the model was based upon the putative binding site as determined via photoaffinity labeling with novobiocin analogues subjected to LC-MS/MS (liquid chromatography-mass spectrometry/mass spectrometry). The bioactive conformation of novobiocin was docked to the SAXS (small-angle X-ray scattering) structure of

HtpG (*Escherichia coli* Hsp90) and subjected to ligand-supported refinement and subsequent systematic molecular dynamics (MD) to attain a homology model. Examination of the potential PTMs within the putative binding domain were conducted in light of recently published data by Hart *et al.*. Hart and coworkers isolated Hsp90 via immunaffinity chromatography (using an *O*-GlcNAc-specific antibody) followed by LC-MS/MS and demonstrated that Hsp90 can be *O*-GlcNAcylated in non-treated rat brain extracts.[5] However, this study did not identify which specific residues were modified, nor address its impact upon Hsp90 activity. In fact, no further studies have been published that analyze the effects of this PTM on Hsp90. It's possible that Hsp90 may be subject to *O*-GlcNAcylation under hyperglycemic stress. As mentioned previously, *O*-GlcNAcylation tends to function more in deactivation versus activation associated with phosphorylation. Hence, this PTM may adversely impact the ability of Hsp90 to function properly. Additionally, Hsc70 and inducible Hsp70 possess lectin attributes.[6-7] Their associations with Hsp90 within the heteroprotein folding complex may be altered as well. If KU-32 occupies the C-terminal nucleotide-binding site, access of OGT (*O*-GlcNAc Transferase) to these potential PTM-sites may be restricted, preventing the accumulation of potentially dysfunctional Hsp90.

As reviewed in section I, Hsp70 assimilates into a multitude of complexes that assist in triaging Hsp90 and Hsp70 client proteins, degrading irreparable proteins, molecular transport, and several specialized neuronal functions through neural J protein interactions. Several of these potential involvements are currently being

investigated within collected samples from both *in vitro* and *in vivo* studies. The relatively indiscriminate improvements in MNCV, SNCV, and large myelinated and small unmyelinated nerve fiber sensation suggests that the compound may regulate propagation and/or neurotransmitter vesicle cycling. Indeed, Hsp70/Hsc70 interchangeability with the neural J proteins provides multiple avenues of plausible neuroprotection.

Equally important, Hsp70 may also assist in maintaining mitochondrial integrity during hyperglycemia-induced oxidative/nitrosative stress. Axons require high concentrations of mitochondria to operate efficiently. In addition to potential upregulation of antioxidant defense mechanisms, such as Mn/CuSOD (Hsp90 client proteins), Hsp90 and Hsp70 facilitate the delivery of preproteins to the mitochondrial membrane transporter TOM70.[8-9] TOM70 imports these preproteins into the mitochondria, where mtHsp70 (mitochondrial Hsp70) shuttles them to Hsp60 for subsequent folding into their mature conformations.[8-9] Preliminary proteomic data involving KU-32-treated Schwann cells and recent *in vitro* data collected from purified DRGs suggests that KU-32-treatment enhances Hsp60 expression. The affects of induced Hsp60 expression are two-fold: Not only does it facilitate folding/refolding of proteins within the mitochondria, but it also sequesters Bax in the cytosol.[10-12] When Bax dissociates, it reallocates to the outer membrane of the mitochondria, pries open the mitochondrial channels, releases cytochrome c, and enables caspase-mediated apoptosis.[10-12] Hence, Hsp60 expression also inhibits the intrinsic apoptotic pathway and, thereby, prevents stress-induced neuronal death.

As Hsp60 is not inducible with the heat shock response, Hsp70 and/or Hsp90 must have additional interactions with Hsp60 or its regulatory mechanisms. This regulation returns back to the post-translational affects of *O*-GlyNAcylation. As discussed in section I, *O*-GlcNAcylation activates p53, inducing pro-apoptotic gene expression, and deactivates c-*myc*, reducing pro-survival transcription.[12-14] As it turns out, c-*myc* regulates Hsp60 expression and p53 regulates Bax expression.[12, 15] Furthermore, hyperglycemic β-cells induce the expression of *O*-GlcNAc-Hsp60 two-fold, inducing Bax release and β-cell death.[16] Hence, *O*-GlcNAcylation may significantly amplify the pathophysiology of DPN. However, p53 and c-*myc* are both Hsp90 client proteins and, therefore, can be induced via Hsp90/Hsp70 expression.[4, 12, 17-19] The lectin properties of Hsp70 may also enable it to bind *O*-GlcNAc-Hsp60, possibly preventing Hsp60 proteolytic degradation and/or stabilizing the *O*-GlcNAc-Hsp60-Bax complex.[5-7, 16, 20-24]

Immunoblot analyses also revealed the downregulation of nNOS (neuronal nitric oxide synthase) in WT 12-week intervention studies. However, it must be noted that preliminary *in vitro* studies of purified neonatal DRGs (murine), differentiated neuroblastoma cells, and transient *in vivo* mouse studies display a prompt induction of nNOS. Therefore, the observed reduction in nNOS expression at the conclusion of the intervention study may not adequately reflect the transient affects instilled by KU-32. Contrary to the afore mentioned detrimental effects of nitric oxide, controlled nitric oxide production by select NOS isoforms is essential for neuronal function and maintaining vascular tone. NO is an essential neurotransmitter within the peripheral

nervous system. Malfunctions in eNOS (endothelial NOS) and iNOS (inducible NOS) have been implicated in neuropathic development.[25] However, the specific involvement of nNOS is not as well understood. The mechanism for NO production is shown in Figure 5.2.

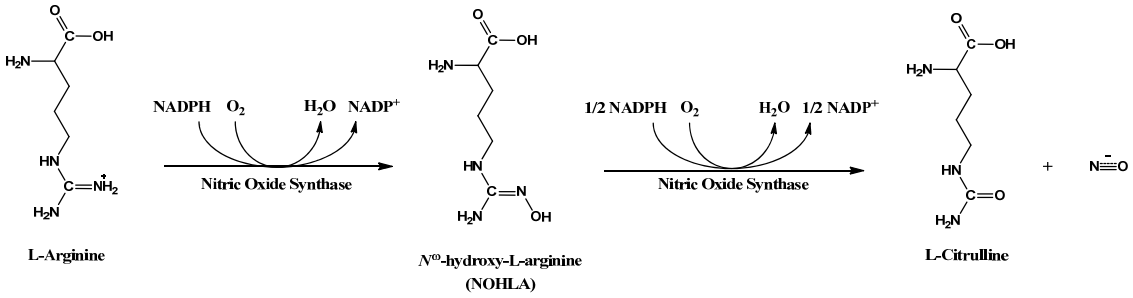

Figure 5.2. Synthesis of nitric oxide via nitric oxide synthase and L-arginine.

NOS employs NADPH and O_2 to conduct two monooxygenation reactions to convert L-arginine to L-citrulline and nitric oxide. The formation of a calcium-calmodulin (Ca^{2+}-CaM) complex facilitates the dimerization of NOS monomers, which each contain one reductase and oxygenase domain.[26] Hsp90 acts as an allosteric activator of nNOS and eNOS, enhancing calmodulin's binding affinity for NOS and increasing dimerization.[27-29] iNOS, implicated in diabetes, is expressed in virtually all tissues and exhibits a much higher binding affinity for calmodulin relative to nNOS and eNOS.[30] Hence, Hsp90 (and Hsp70) may serve to stabilize nNOS:calmodulin interactions in the face of excess iNOS concentrations. Obrosova and coworkers demonstrated that peripheral nerves require functional nNOS to sustain normal functions and regulate sensory nerve fiber innervation.[25] They also showed that nNOS knockout mice expressed significant decreases in NCV, mechanical

response, and IENFD.[25] Therefore, the potential increase in stabilized nNOS (via Hsp90) may serve to renormalize essential neuronal communication processes. In addition, increasing Hsp60 and Hsp70 expression within the rostral ventrolateral medulla (RVLM) generate selective upregulation of the pro-survival nNOS/Protein Kinase G (PKG) signaling pathways (independent of Hsp90) while simultaneously reducing iNOS/peroxynitrite formation.[31] PKG helps to regulate calcium flux into the neuron. Thus, Hsp90, Hsp70, and Hsp60 induction may restore normal nNOS function and reduce pathological iNOS activity.

It's also worth noting that several of the novobiocin-based Hsp90 inhibitors not only disrupt the Hsp90 heteroprotein complexes, but may also alter the expression of other Hsp90 family members (Grp94 and Trap-1) as evidenced through preliminary immunoblot analyses (data not shown). It's proposed that upregulation of these two isoforms may be a compensatory mechanism when Hsp90 is rendered dysfunctional. Grp94 is involved with the unfolded protein response and guides initial protein folding within the rough endoplasmic reticulum.[32] Ubiquitination of irreparable proteins by Hsp70 in DPN may clear damaged proteins to "make room" for newly synthesized, functional proteins. The specific functions of Trap-1 within the mitochondria remain largely unknown.

II. CONCLUSION

In summary, the potential for Hsp90 and Hsp70 involvement in KU-32-induced neuroprotection is far-reaching and requires additional investigation to elucidate the compound's specific mechanism of action. Regardless, KU-32 displays

remarkable efficacy and these studies provide proof-of-principal that C-terminal Hsp90 modulators can ameliorate neuron degeneration in diabetic peripheral neuropathy.

III. References

1. Burlison, J. A.; Neckers, L.; Smith, A. B.; Maxwell, A.; Blagg, B. S., *J Am Chem Soc* **2006,** *128* (48), 15529-36.

2. Burlison, J. A.; Avila, C.; Vielhauer, G.; Lubbers, D. J.; Holzbeierlein, J.; Blagg, B. S., *J Org Chem* **2008,** *73* (6), 2130-7.

3. Marcu, M. G.; Chadli, A.; Bouhouche, I.; Catelli, M.; Neckers, L. M., *J Biol Chem* **2000,** *275* (47), 37181-6.

4. Donnelly, A.; Blagg, B. S., *Curr Med Chem* **2008,** *15* (26), 2702-17.

5. Wells, L.; Vosseller, K.; Cole, R. N.; Cronshaw, J. M.; Matunis, M. J.; Hart, G. W., *Mol Cell Proteomics* **2002,** *1* (10), 791-804.

6. Guinez, C.; Lemoine, J.; Michalski, J. C.; Lefebvre, T., *Biochem Biophys Res Commun* **2004,** *319* (1), 21-6.

7. Guinez, C.; Losfeld, M. E.; Cacan, R.; Michalski, J. C.; Lefebvre, T., *Glycobiology* **2006,** *16* (1), 22-8.

8. Hood, D. A.; Adhihetty, P. J.; Colavecchia, M.; Gordon, J. W.; Irrcher, I.; Joseph, A. M.; Lowe, S. T.; Rungi, A. A., *Med Sci Sports Exerc* **2003,** *35* (1), 86-94.

9. Young, J. C.; Hoogenraad, N. J.; Hartl, F. U., *Cell* **2003,** *112* (1), 41-50.

10. Cappello, F.; Conway de Macario, E.; Marasa, L.; Zummo, G.; Macario, A. J., *Cancer Biol Ther* **2008,** *7* (6), 801-9.

11. Arya, R.; Mallik, M.; Lakhotia, S. C., *J Biosci* **2007,** *32* (3), 595-610.

12. Weinberg, R. A., *The biology of cancer*. Garland Science: New York, NY, 2007; p 1 v. (various pagings).

13. Fiordaliso, F.; Leri, A.; Cesselli, D.; Limana, F.; Safai, B.; Nadal-Ginard, B.; Anversa, P.; Kajstura, J., *Diabetes* **2001,** *50* (10), 2363-75.

14. Chou, T. Y.; Hart, G. W.; Dang, C. V., *J Biol Chem* **1995,** *270* (32), 18961-5.

15. Tsai, Y. P.; Teng, S. C.; Wu, K. J., *FEBS Lett* **2008,** *582* (29), 4083-8.

16. Kim, H. S.; Kim, E. M.; Lee, J.; Yang, W. H.; Park, T. Y.; Kim, Y. M.; Cho, J. W., *FEBS Lett* **2006,** *580* (9), 2311-6.

17. Picard, D. Hsp90 Interactors. 2010. www.picard.ch/downloads/Hsp90interactors.pdf (accessed June 2010).

18. Pratt, W. B.; Toft, D. O., *Exp Biol Med (Maywood)* **2003,** *228* (2), 111-33.

19. Whitesell, L.; Lindquist, S. L., *Nat Rev Cancer* **2005,** *5* (10), 761-72.

20. Butkinaree, C.; Park, K.; Hart, G. W., *Biochim Biophys Acta* **2010,** *1800* (2), 96-106.

21. Lefebvre, T.; Cieniewski, C.; Lemoine, J.; Guerardel, Y.; Leroy, Y.; Zanetta, J. P.; Michalski, J. C., *Biochem J* **2001,** *360* (Pt 1), 179-88.

22. Zachara, N. E.; O'Donnell, N.; Cheung, W. D.; Mercer, J. J.; Marth, J. D.; Hart, G. W., *J Biol Chem* **2004,** *279* (29), 30133-42.

23. Walgren, J. L.; Vincent, T. S.; Schey, K. L.; Buse, M. G., *Am J Physiol Endocrinol Metab* **2003,** *284* (2), E424-34.

24. Hu, P.; Shimoji, S.; Hart, G. W., *FEBS Lett* **2010,** *584* (12), 2526-2538.

25. Vareniuk, I.; Pacher, P.; Pavlov, I. A.; Drel, V. R.; Obrosova, I. G., *Int J Mol Med* **2009,** *23* (5), 571-80.

26. Zhou, L.; Zhu, D. Y., *Nitric Oxide* **2009,** *20* (4), 223-30.

27. Song, Y.; Cardounel, A. J.; Zweier, J. L.; Xia, Y., *Biochemistry* **2002,** *41* (34), 10616-22.

28. Song, Y.; Zweier, J. L.; Xia, Y., *Biochem J* **2001,** *355* (Pt 2), 357-60.

29. Song, Y.; Zweier, J. L.; Xia, Y., *Am J Physiol Cell Physiol* **2001,** *281* (6), C1819-24.

30. Kone, B. C.; Kuncewicz, T.; Zhang, W.; Yu, Z. Y., *Am J Physiol Renal Physiol* **2003,** *285* (2), F178-90.

31. Chan, J. Y.; Cheng, H. L.; Chou, J. L.; Li, F. C.; Dai, K. Y.; Chan, S. H.; Chang, A. Y., *J Biol Chem* **2007,** *282* (7), 4585-600.

32. Hotamisligil, G. S., *Cell* **2010,** *140* (6), 900-17.